

Custodial Leptons and Higgs Decays

Adrián Carmona and Florian Goertz

*Institute for Theoretical Physics,
ETH Zurich, 8093 Zurich, Switzerland*

E-mail: carmona@itp.phys.ethz.ch, fgoertz@itp.phys.ethz.ch

ABSTRACT: We study the effects of extended fermion sectors, respecting custodial symmetry, on Higgs production and decay. The resulting protection for the $Z \rightarrow b_L b_L$ and $Z \rightarrow \tau_R \tau_R$ decays allows for potentially interesting signals in Higgs physics, while maintaining the good agreement of the Standard Model with precision tests, without significant fine-tuning. Although being viable setups on their own, the models we study can particularly be motivated as the low energy effective theories of the composite Higgs models MCHM₅ and MCHM₁₀ or the corresponding gauge-Higgs unification models. The spectra can be identified with the light custodians present in these theories. These have the potential to describe the relevant physics in their fermion sectors in a simplified and transparent way. In contrast to previous studies of composite models, we consider the impact of a realistic lepton sector on the Higgs decays. We find significant modifications in the decays to τ leptons and photons due to the new leptonic resonances. While from a pure low energy perspective an enhancement of the channel $pp \rightarrow h \rightarrow \gamma\gamma$ turns out to be possible, if one considers constraints on the parameters from the full structure of the composite models, the decay mode into photons is always reduced. We also demonstrate that taking into account the non-linearity of the Higgs sector does not change the qualitative picture for the decays into τ leptons or photons in the case of the dominant Higgs production mechanism.

Contents

1	Introduction	1
2	Low Energy Spectrum and Higgs Couplings of the Models	3
2.1	MCHM ₅	4
2.2	MCHM ₅₊₁₀	7
3	Higgs Production and Decay	8
3.1	General Structure	8
3.2	Explicit Results in the Models at Hand	11
3.2.1	MCHM ₅	11
3.2.2	MCHM ₅₊₁₀	13
3.3	Phenomenological Implications	18
3.4	Impact of the Non-Linearity of the Higgs	24
4	Conclusions	26
A	Form Factors	29

1 Introduction

Recently, a new boson has been discovered in both the ATLAS [1] and CMS [2] experiments at the Large Hadron Collider (LHC). It is still to be confirmed that this particle is the long-sought Higgs boson, the last missing ingredient of the Standard Model (SM) of Particle Physics. While the overall picture of the measured cross sections in its various decay channels is in reasonable agreement with the SM-Higgs expectations, there is also still room for significant deviations. In particular, both experiments observe a tendency towards an enhanced decay into two photons, at the level of 1-2 σ . Moreover, although the trend for a depletion in the decay-channel into τ leptons has become less strong, a reduced rate in that mode still fits well with the data - the ATLAS results are still compatible with a vanishing signal at the level of about 1 σ [3, 4].

These trends might vanish after more statistics has been accumulated, however it is always worth studying the impact of extensions of the SM on Higgs physics, to examine to what extent they could agree with experimental tendencies or to constrain these models. The most straightforward way to enhance for example the two-photon signal without affecting other channels too much is to add new leptons to the SM with Higgs couplings that are not aligned to their masses. This opens the possibility of a constructive interference of the new leptons in the loop contributing to $h \rightarrow \gamma\gamma$ with the W^\pm boson loop. This option has been considered in [5, 6]. In general, many models involving new particles have been

introduced to account for the enhancement in the photon channel, some without embedding the new physics into a motivated UV completion, others studying $h \rightarrow \gamma\gamma$ in (more) complete models, addressing the hierarchy problem of particle physics [5–49].

In this paper we want to consider, on the one hand, simple low-energy models featuring new quarks and leptons, that allow to clearly keep track of the observed effects in Higgs physics. On the other hand we also try to address the question where the new particles could come from, thereby increasing the predictivity of the setup. Most importantly, we are led by the request to keep the good agreement of the SM with precision tests also for the extended setup, without introducing severe fine-tuning. To that extend, we embed the new physics sector in a way that respects a custodial symmetry protecting the T parameter as well as the couplings of the Z boson to fermions. Such a symmetry is likely to be an ingredient of viable new-physics models at the TeV scale.

To be specific, we study two realizations of an extended fermion sector, one featuring fundamental representations of $SO(5)$, the other employing also an adjoint (ten-dimensional) representation of the same Lie-group, which both possess a custodial $SU(2)_L \times SU(2)_R \times P_{LR} (\subset SO(5))$ symmetry. Although being valid setups on their own, they are particularly motivated as the low energy tails of minimal composite Higgs models (MCHM) or corresponding models of gauge-Higgs unification (GHU) [50–55].

Such models lead generically to the presence of light resonances associated to the top quark and required by custodial symmetry [56–62], with masses significantly below the actual scale of these models, $m_{\text{cust}} \ll f$. This is a consequence of the large value of the top mass and the enlarged fermion representations chosen to protect the $Zb\bar{b}$ vertex from anomalous corrections. Looking at the value of the lepton masses, there is *a priori* no reason to think that something analogous could happen in the lepton sector. However, as it was shown in [63], trying to explain the observed pattern of lepton masses and mixings with the help of a discrete A_4 symmetry requires the τ to be more composite than naively expected and thus makes the appearance of light τ custodians quite likely. Phenomenological consequences of such resonances at the LHC were also studied in detail in [64]. Although the presence of τ custodians was predicted in [63] just for the MCHM₅, where all the leptons are in fundamental representations of $SO(5) \times U(1)_X$, they are also present when we choose larger representations for the charged leptons [65]. Therefore, finding light τ custodians at the LHC, directly or through the modifications induced on the different Higgs decays, could be interpreted as a strong hint for the compositeness of the recently discovered Higgs boson.

At low energies $E \ll f$ one would see the SM plus resonances coming with the top quark and the τ lepton, which just corresponds to what we will be studying in this article. The impact of possible UV completions on the parameters of the models will be detailed further below. We will use the abbreviations MCHM₅ (MCHM₅₊₁₀) for these extended fermion sectors featuring **5**s (**5**s plus one **10**) of $SO(5)$, although we will not consider the full composite models, *i.e.* we will neglect heavier fermionic resonances, possible changes in the gauge-boson sector and for the first part of the analysis also the effects from the non-linearity of the Higgs sector. We will however study the impact of the latter effect at the end of the article. Note that, in what we call the MCHM₅₊₁₀, we will only embed

the τ_R in a $\mathbf{10}$, whereas the other fermions will remain in the fundamental representation of $SO(5)$. Due to the significant compositeness of the τ lepton one expects non-negligible effects in the lepton sector of Higgs physics, which have been neglected so far. It would be interesting to consider these effects also in complete composite Higgs models. A detailed examination of this is left for future work [65]. However, as we will explain below, the simplified setup of our analysis will already grasp the most important structure of these effects in a very transparent way and moreover is also valid in a more general context.

In Section 2, we will detail the extended fermion sectors studied in this work and derive the corresponding spectra and Higgs couplings. The anatomy of the Higgs-production and decay cross sections in the models at hand will be studied in Section 3, where we also give numerical predictions for various search channels. Finally, our conclusions will be presented in Section 4.

2 Low Energy Spectrum and Higgs Couplings of the Models

The emergence of light leptonic custodians in the MCHM₅ has been motivated in [63] from a UV perspective for a complete composite Higgs model, and similar considerations hold, putting the τ_R into a $\mathbf{10}$ of $SO(5)$ [65]. However, as mentioned before, the setup for our analysis of Higgs production and decay will only be the corresponding low energy theory, including the light custodians. Beyond that, we do not even have to rely on a certain UV completion of this model but rather consider it as a general low energy setup featuring a viable implementation of custodial protection, with the only additional assumption being that the scale of a possible UV completion is significantly larger than the mass-scale of the new fermionic resonances considered. The particle spectrum is then inspired by the prominent role of the third fermion generation. This will be the starting point for our analysis.

In the case we do want to consider a model of GHU (or composite Higgs) completing this setup and causing the existence of the light resonances, this has however to be taken with a grain of salt. The 5D structure of this model leads to relations between different Kaluza-Klein (KK) modes of the same level such that the suppressed contributions of modes with masses significantly larger than the light custodians can be lifted by relatively larger Yukawa couplings in the triangle diagrams examined in Section 3. To consider really the full structure of the fermion sectors of these models at leading order, it seems important to take into account complete KK levels.¹ In the models that we will study, this is indeed assured (effectively). In one case, those heavy resonances, that are missing to complete the KK level of the light custodians that we consider, will have negligible couplings to the Higgs boson. In the other, it turns out that already those modes present in our low energy setup exhibit the structure that describes the full KK structure. The former is true for the Y sector in the MCHM₅₊₁₀, while the latter happens for the top, bottom and τ sectors. We will elaborate more on this further below. We now leave again the question of a possible UV completion for the next considerations.

¹Note that in full 5D models all leptons live in representations of $SO(5)$.

In choosing how to embed the SM fermion sector in enlarged representations, we are led by the assumption that the (right handed) top quark plays a special role in the fermion sector and that thus the new light resonances should complete the right handed top to form a representation under $SO(5)$ and that the same could hold for the right handed τ sector. The assumption that (only) those two SM fermions couple strongly to the new sector will also constrain the ranges that we will chose for the parameters of the models, see below.

In consequence, the setup we want to consider for the following analysis corresponds to the SM Lagrangian, supplemented only with vector-like fermions, associated to the top and τ sectors, that live in fundamental or adjoint representations of $SO(5)$, such that there is a custodial protection for $Z \rightarrow b_L b_L$ as well as $Z \rightarrow \tau_R \tau_R$ decays (which is important due to the non-negligible mixings with the new sector). We will now give the details of this setup, with the focus on the spectrum and the Higgs couplings. We start with the option of putting the fermions in the fundamental representation of $SO(5)$. As mentioned, we will call this setup MCHM₅ in the following, although for us it is only the low energy theory, featuring fermions in the fundamental representation of $SO(5)$ and not a complete composite model. For the lepton sector, this model has been studied in [64] and we will give a short review of the key features in the following, generalizing the setup to include quarks [66, 67]. After that we will spell out the low energy theory corresponding to the option of putting fermions in the adjoint representation, a **10** of $SO(5)$ (MCHM₁₀).

2.1 MCHM₅

The light τ custodians present in this model in addition to the SM fermions are contained in the lepton-multiplets [64]

$$L_{1L,R}^{(0)} = \begin{pmatrix} N_{1L,R}^{(0)} \\ E_{1L,R}^{(0)} \end{pmatrix} \sim \mathbf{2}_{-\frac{1}{2}}, \quad L_{2L,R}^{(0)} = \begin{pmatrix} E_{2L,R}^{(0)} \\ Y_{2L,R}^{(0)} \end{pmatrix} \sim \mathbf{2}_{-\frac{3}{2}}, \quad (2.1)$$

where the given transformation properties correspond to $(SU(2)_L)_Y$ and the $SU(2)_R$ quantum numbers are $T_R^3 = 1/2$ and $T_R^3 = -1/2$, respectively, following from the embedding in the full $SO(5) \times U(1)_X$ gauge group. The superscript (0) indicates the current basis. The model is designed such that the custodial symmetry protects the $Z\tau_R\tau_R$ coupling (see [68]). In addition, we assume a similar embedding of the quark sector, now featuring a protection for the Zb_Lb_L coupling. This is achieved by a setup which, due to the large top mass, leads to the light custodians

$$Q_{1L,R}^{(0)} = \begin{pmatrix} \Lambda_{1L,R}^{(0)} \\ T_{1L,R}^{(0)} \end{pmatrix} \sim \mathbf{2}_{\frac{7}{6}}, \quad Q_{2L,R}^{(0)} = \begin{pmatrix} T_{2L,R}^{(0)} \\ B_{2L,R}^{(0)} \end{pmatrix} \sim \mathbf{2}_{\frac{1}{6}}. \quad (2.2)$$

The Lagrangian of our model consists of the SM operators, supplemented with all possible gauge invariant combinations involving the new fermion multiplets. Neglecting the first two generations, which are assumed to have negligible couplings to the new resonances, the mass and Yukawa couplings are given by

$$\mathcal{L}_L = -y_l \bar{l}_L^{(0)} \varphi \tau_R^{(0)} - y'_l \left[\bar{L}_{1L}^{(0)} \varphi + \bar{L}_{2L}^{(0)} \tilde{\varphi} \right] \tau_R^{(0)} - M_l \left[\bar{L}_{1L}^{(0)} L_{1R}^{(0)} + \bar{L}_{2L}^{(0)} L_{2R}^{(0)} \right] + \text{h.c.} \quad (2.3)$$

and

$$\mathcal{L}_Q = -y_q \bar{q}_L^{(0)} \varphi t_R^{(0)} - y'_q \left[\bar{Q}_{1L}^{(0)} \varphi + \bar{Q}_{2L}^{(0)} \tilde{\varphi} \right] t_R^{(0)} - M_Q \left[\bar{Q}_{1L}^{(0)} Q_{1R}^{(0)} + \bar{Q}_{2L}^{(0)} Q_{2R}^{(0)} \right] + \text{h.c.}, \quad (2.4)$$

where $l_L^{(0)}$ and $\tau_R^{(0)}$ ($q_L^{(0)}$ and $t_R^{(0)}$) denote the third generation SM leptons (quarks). After electroweak symmetry breaking (EWSB) and in unitary gauge, the Higgs doublet is given by $\varphi = 1/\sqrt{2}(0, v+h)^T$, with $v = 246$ GeV and h the Higgs boson, whereas $\tilde{\varphi} = i\sigma_2 \varphi^*$. Note that we neglected the couplings of the right handed bottom quark (or the corresponding neutrino), which are SM like since there are no new resonances to which it could couple, due to the charges and multiplet structure of the MCHM₅. The fact that different operators above have the same Yukawa couplings or vector-like masses is due to the P_{LR} symmetry, exchanging $SU(2)_L \leftrightarrow SU(2)_R$.

The model is simple enough that compact analytical formulas can be derived for the physical masses and Higgs couplings of the extended fermion sector, which we will give here for the leptons. For the quarks, the same formulas hold with the replacements $\tau \rightarrow t, E \rightarrow T, Y \rightarrow B$, and $N \rightarrow \Lambda$ and we will suppress indices if convenient. The only non-trivial fermion mass matrix (featuring non-vanishing Yukawa couplings) that follows from (2.3) belongs to the E (T) sector and reads

$$\mathcal{M}^5 = \frac{v}{\sqrt{2}} \begin{pmatrix} y & 0 & 0 \\ y' & \frac{\sqrt{2}}{v} M & 0 \\ y' & 0 & \frac{\sqrt{2}}{v} M \end{pmatrix}. \quad (2.5)$$

Let us already make a first comment on the expected size of the entries of this matrix. Our working assumption is that the top-quark and the τ lepton couple significantly, with a strength governed by the electroweak scale v , to the new physics and thus we expect $y' \sim 1$. The parameter y describes the mass term between the SM-like top (or τ) fields and is thus governed to a large extent by their mass eigenvalues. The vector-like masses of the new resonances associated to the top and τ sectors are, motivated by the exposed role of these fermions, expected to be significantly smaller than the general scale of new physics, *i.e.*, $\mathcal{O}(\text{TeV}) \gg M \gg v$.

From the explicit perspective of a composite model for example, one expects the vector-like mass M to be lighter than the scale of compositeness $f \gg M \gg v$. The Yukawa coupling y parametrizes the interactions of the right handed τ and t , which have a sizable composite component, with the composite Higgs boson and their more elementary left-handed components, whereas y' describes interactions of the τ_R or t_R with heavy composite resonances and the composite Higgs. In consequence both mass-couplings are non negligible, however one still expects typically $v y \ll v y' \ll M$, where the first “ \ll ” should rather be a “ $<$ ” for the top-quark sector. Remember that the flavor pattern of composite Higgs models (featuring partial compositeness) matches nicely with the experimental observation that possible deviations from the SM in the third generation of fermions are less severely constrained. Beyond these considerations, note that already from the pure fact that no additional fermions have been found at the LHC yet, one expects $M \gg v$ (see

(2.8) below). We will use such insights on hierarchies in choosing the parameter-space for our scans in Section 3.3.

The matrix (2.5) can be diagonalized via a bi-unitary transformation, $U_L^{5\dagger} \mathcal{M}^5 U_R^5 = \mathcal{M}_{\text{diag}}^5 = (m_\tau, m_{E_1}, m_{E_2})$, which due to the structure of (2.5) takes the simple form

$$U_{L,R}^5 = \begin{pmatrix} c_{L,R} & 0 & s_{L,R} \\ -\frac{s_{L,R}}{\sqrt{2}} & \frac{1}{\sqrt{2}} & \frac{c_{L,R}}{\sqrt{2}} \\ -\frac{s_{L,R}}{\sqrt{2}} & -\frac{1}{\sqrt{2}} & \frac{c_{L,R}}{\sqrt{2}} \end{pmatrix}, \quad (2.6)$$

with the sine and cosine of the mixing angles $s_{L,R} \equiv \sin(\theta_{L,R})$, $c_{L,R} \equiv \cos(\theta_{L,R})$. The relevant input parameters of the model at this point are y , y' and M . However, it will be more convenient to use as input m_τ , s_R , and M , where the first quantity is already fixed by experiment. The left-handed mixing parameter is related to them via

$$s_L = s_R \frac{m_\tau}{M}. \quad (2.7)$$

The physical non-SM states consist of three heavy particles of degenerate vector-like mass

$$m_N = m_{E_1} = m_Y = M, \quad (2.8)$$

and electric charges of $Q = 0, -1, -2$ ($Q = 5/3, 2/3, -1/3$) in the lepton (quark) sector. In addition, there is a heavier $Q = -1$ ($Q = 2/3$) state with

$$m_{E_2} = \frac{M}{c_R} \sqrt{1 - s_R^2 \frac{m_\tau^2}{M^2}}. \quad (2.9)$$

The couplings of the fermions to the Higgs boson are given by

$$\mathcal{L}_h = \sum_{f=E,T} \bar{\Psi}_L^{f5(0)} g_{h5}^{f(0)} \Psi_R^{f5(0)} h + \text{h.c.}, \quad (2.10)$$

where $\Psi^{E5(0)} \equiv (\tau^{(0)}, E_1^{(0)}, E_2^{(0)})^T$, $\Psi^{T5(0)} \equiv (t^{(0)}, T_1^{(0)}, T_2^{(0)})^T$ and

$$\sqrt{2} g_{h5}^{f(0)} = \begin{pmatrix} y & 0 & 0 \\ y' & 0 & 0 \\ y' & 0 & 0 \end{pmatrix}. \quad (2.11)$$

After rotating to the diagonal mass basis, the Higgs-coupling matrix with leptons becomes

$$g_{h5}^E = U_L^{5\dagger} g_{h5}^{E(0)} U_R^5 = \frac{1}{v} \begin{pmatrix} c_R^2 m_\tau & 0 & s_R c_R m_\tau \\ 0 & 0 & 0 \\ s_R c_R M_{E_2} & 0 & s_R^2 M_{E_2} \end{pmatrix}, \quad (2.12)$$

and similarly for the quark sector. It features off-diagonal entries, due to the presence of the vector-like masses M . Note that in the MCHM₅ the new resonances belonging to the N, Y, Λ, B sectors do not couple to the Higgs, as one can not write a gauge invariant term mediating such a coupling.

2.2 MCHM₅₊₁₀

It is easy to show that, analogously to the discussion in [63], embedding the τ_R in an adjoint representation of $SO(5)$ and requiring a custodial protection for the $Z\tau_R\tau_R$ coupling leads to the following light custodians [65], belonging to a **10** of $SO(5)$,²

$$L_{1L,R}^{(0)} = \begin{pmatrix} N_{1L,R}^{(0)} \\ E_{1L,R}^{(0)} \end{pmatrix} \sim \mathbf{2}_{-\frac{1}{2}}, \quad L_{2L,R}^{(0)} = \begin{pmatrix} E_{2L,R}^{(0)} \\ Y_{2L,R}^{(0)} \end{pmatrix} \sim \mathbf{2}_{-\frac{3}{2}}, \quad (2.13)$$

$$L_{3L,R}^{(0)} = \begin{pmatrix} N_{3L,R}^{(0)} \\ E_{3L,R}^{(0)} \\ Y_{3L,R}^{(0)} \end{pmatrix} \sim \mathbf{3}_{-1}, \quad N_{2L,R}^{(0)} \sim \mathbf{1}_0, \quad Y_{1L,R}^{(0)} \sim \mathbf{1}_{-2}. \quad (2.14)$$

Note that we will keep the other lepton multiplets, as well as the quarks, in the fundamental representation.³ As a consequence, we do not give the quark sector for the **10**, which can however be worked out straightforwardly. This setup can be seen as the most straightforward departure from the MCHM₅ and, as we will detail further below, a first step towards the embedding of all SM fermions into **10**s of $SO(5)$ in a GHU model, while still describing the full fermion sector of the composite model by the light custodians in a simple and self-contained way.

Here, again, the superscript (0) indicates the current basis and the $SU(2)_R$ quantum numbers are $T_R^3 = 1/2, -1/2$ for the two $SU(2)_L$ doublets, whereas the $SU(2)_L$ triplets are $SU(2)_R$ singlets and vice versa. The relevant part of the Yukawa and mass Lagrangian now reads⁴

$$\begin{aligned} \mathcal{L} = & -y \bar{l}_L^{(0)} \varphi \tau_R^{(0)} - y' \left[\bar{L}_{1L}^{(0)} \varphi + \bar{L}_{2L}^{(0)} \tilde{\varphi} \right] \tau_R^{(0)} - M \left[\bar{L}_{1L}^{(0)} L_{1R}^{(0)} + \bar{L}_{2L}^{(0)} L_{2R}^{(0)} \right] \\ & - \tilde{M} \left[\bar{L}_{3L}^{(0)} L_{3R}^{(0)} + \bar{Y}_{1L}^{(0)} Y_{1R}^{(0)} \right] - \tilde{y} \bar{l}_L^{(0)} \sigma^I \varphi L_{3R}^{(0)I} - \hat{y} \left[\bar{L}_{1L}^{(0)} \sigma^I \varphi - \bar{L}_{2L}^{(0)} \sigma^I \tilde{\varphi} \right] L_{3R}^{(0)I} \\ & - \sqrt{2} \tilde{y} \bar{L}_{2L}^{(0)} \varphi Y_{1R}^{(0)} + \bar{y}^* \left[\bar{L}_{1R}^{(0)} \sigma^I \varphi - \bar{L}_{2R}^{(0)} \sigma^I \tilde{\varphi} \right] L_{3L}^{(0)I} + \sqrt{2} \bar{y}^* \bar{L}_{2R}^{(0)} \varphi Y_{1L}^{(0)} + \text{h.c.} \end{aligned} \quad (2.15)$$

After EWSB, we obtain the mass matrices

$$\mathcal{M}_E = \frac{v}{\sqrt{2}} \begin{pmatrix} y & 0 & 0 & -\tilde{y} \\ y' & \frac{\sqrt{2}}{v} M & 0 & -\hat{y} \\ y' & 0 & \frac{\sqrt{2}}{v} M & -\hat{y} \\ 0 & \bar{y} & \bar{y} & \frac{\sqrt{2}}{v} \tilde{M} \end{pmatrix}, \quad \mathcal{M}_Y = v \begin{pmatrix} \frac{1}{v} \tilde{M} & -\bar{y} & 0 \\ \hat{y} & \frac{1}{v} M & -\hat{y} \\ 0 & \bar{y} & \frac{1}{v} \tilde{M} \end{pmatrix}, \quad (2.16)$$

for the $Q = -1, -2$ leptons, respectively. Again, the natural size of the parameters appearing in (2.16) can be motivated from the expected degree of compositeness of the contributing particles, determining the overlap and thus the mass-mixings or more general considerations. We will give the ranges of parameters that we employ in Section 3.2.

²With some abuse of notation, we use the same names as already used for the MCHM₅. However, the assignment will be clear from the context.

³For the low energy Lagrangian of the light custodians, given in this section, the embedding of the first two generations is irrelevant.

⁴Note that we will neglect the neutrino sector, as it is irrelevant for the following discussions.

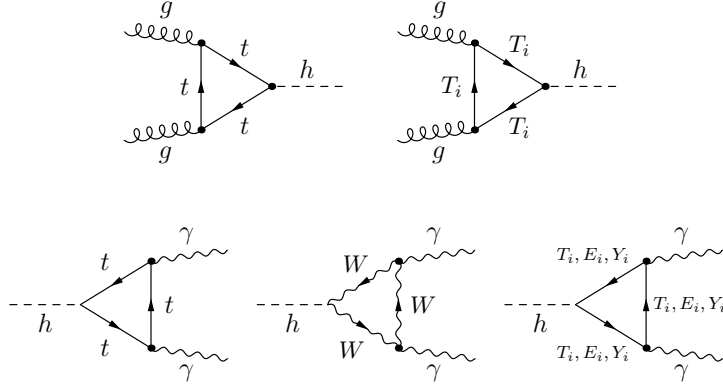


Figure 1. First row: Leading-order contribution to Higgs-boson production via gluon-gluon fusion and contribution from heavy quark resonances to the same process; Second row: Leading contributions to the Higgs decay into two photons, given by a top-quark loop and a W^\pm -boson loop, as well as contributions from heavy fermion resonances to the same process.

The rotations to the mass basis will be in analogy to (2.6), but now featuring larger matrices. We will resort to numerical methods for these diagonalizations in the following. Note that, if we are only interested in sums of ratios of Higgs couplings over masses, we can arrive at simple analytical expressions, avoiding the diagonalization procedure, see Section 3.

The couplings of the fermions to the Higgs boson are now given by

$$\mathcal{L}_h = \sum_{f=E,Y} \bar{\Psi}_L^{f10(0)} g_{h10}^{f(0)} \Psi_R^{f10(0)} h + \text{h.c.}, \quad (2.17)$$

where

$$\Psi^{E10(0)} \equiv (\tau^{(0)}, E_1^{(0)}, E_2^{(0)}, E_3^{(0)})^T, \quad \Psi^{Y10(0)} \equiv (Y_1^{(0)}, Y_2^{(0)}, Y_3^{(0)})^T, \quad (2.18)$$

and

$$g_{h10}^{f(0)} = \frac{\partial \mathcal{M}_f}{\partial v}, \quad (2.19)$$

with $f = E, Y$. After rotating to the diagonal mass basis, the Higgs-coupling matrices become

$$g_{h10}^f = U_L^{f10\dagger} g_{h10}^{f(0)} U_R^{f10}. \quad (2.20)$$

3 Higgs Production and Decay

3.1 General Structure

The presence of the new resonances has significant implications on the production and decay of the Higgs boson, which will be worked out in this section. The most important production mechanism for the Higgs boson at hadron colliders is gluon-gluon fusion, which in the SM receives its main contribution from a top-quark triangle loop, with a large coupling to the Higgs, see the leftmost diagram in Figure 1. In extensions of the SM this

process can receive corrections from new colored particles that propagate in the loop (see the second diagram in the figure) as well as from modified couplings of the SM quarks in the loop to the Higgs boson. Both effects are present in the models we consider. We parametrize the corresponding deviations by a rescaling factor κ_g^m as

$$\sigma(gg \rightarrow h)_{\text{MCHM}_m} = |\kappa_g^m|^2 \sigma(gg \rightarrow h)_{\text{SM}}, \quad (3.1)$$

whose explicit form will be given further below for $m = 5, 5+10$. Subleading, but nevertheless important, channels for Higgs production at the LHC are vector-boson fusion (VBF) $qq^{(\prime)} \rightarrow qq^{(\prime)}V^*V^* \rightarrow qq^{(\prime)}h$, with $V = W, Z$, associated vector-boson production $q\bar{q}^{(\prime)} \rightarrow V^* \rightarrow Vh$, and associated top-quark pair production $gg \rightarrow t\bar{t}^*t^*\bar{t} \rightarrow t\bar{t}h$, which all appear at the tree level, and the latter two will be abbreviated as Vh and $t\bar{t}h$.⁵ As the theories we consider only change the fermion sector of the SM, the tree-level couplings of the Higgs boson to weak gauge bosons remain standard-model like. The same is true for the couplings of the first two generations of fermions, which, due to their small masses, are assumed to have negligible mixings with the new resonances.⁶ Thus, to leading order,

$$\sigma(\text{VBF})_{\text{MCHM}_m} = \sigma(\text{VBF})_{\text{SM}}, \quad (3.2)$$

$$\sigma(Vh)_{\text{MCHM}_m} = \sigma(Vh)_{\text{SM}}, \quad (3.3)$$

$m = 5, 5+10$. Since gauge invariance guarantees that the couplings of the fermions to the gluon and photon are unchanged, the only correction to associated top-quark pair production in the models at hand arises through the deviation in the $h t\bar{t}$ vertex. The real part of such a coupling of SM-type fermions with the Higgs, $h\bar{f}f$, normalized to the SM, is given by

$$\kappa_f^5 = v \text{Re} [(g_{h5}^F)_{11}] / m_f, \quad (3.4)$$

see (2.10), where $(f, F) = (t, T), (b, B), (\tau, E)$ and

$$\kappa_f^{5+10} = \begin{cases} v \text{Re} [(g_{h10}^F)_{11}] / m_f, & (f, F) = (\tau, E) \\ \kappa_f^5, & f = t, b \end{cases}, \quad (3.5)$$

see (2.17). We then get

$$\sigma(t\bar{t}h)_{\text{MCHM}_m} = (\kappa_t^5)^2 \sigma(t\bar{t}h)_{\text{SM}}, \quad (3.6)$$

$m = 5, 5+10$.

We now turn to the decays of the Higgs boson. The most important modes for a Higgs of $m_h \approx 125 \text{ GeV}$ are $h \rightarrow \gamma\gamma, WW, ZZ, bb, \tau\tau, gg$, where the last one is extremely difficult to measure. Moreover, the decays to two photons or gluons are loop processes, whereas the other decays happen at the tree level. We parametrize deviations from the SM as

$$\Gamma(h \rightarrow ff)_{\text{MCHM}_m} = |\kappa_f^m|^2 \Gamma(h \rightarrow ff)_{\text{SM}}, \quad (3.7)$$

⁵For the anatomy of these processes in the SM, see [69].

⁶In extra dimensional extensions of the SM or composite Higgs models, with anarchic flavor structure, this assumption is motivated by the fact that the first two generations have negligible interactions with the KK excitations, or composite fermions.

$f = \gamma, W, Z, b, \tau, g$. As discussed before, the decay to two vector bosons is unchanged in the models considered

$$\kappa_W^m = \kappa_Z^m = 1, \quad (3.8)$$

$m = 5, 5+10$. Beyond that, the rescaling factors for the (tree-level) decays into two fermions, entering (3.7), have already been specified in (3.4) and (3.5).

In the following, we will derive the explicit structure of the remaining rescaling factors, corresponding to loop precesses, which have not been detailed further yet, *i.e.*, κ_g^m and κ_γ^m . Note that the first one enters in the same form in the gluon-gluon fusion process and in the decay of the Higgs to two gluons. Further below, we will relate the different rescalings to the parameters of the models under consideration.

For the effective coupling to gluons we arrive at

$$\kappa_g^5 = \kappa_g^{5+10} = \frac{\sum_{f=t,b} \kappa_f^5 A_q^h(\tau_f) + \nu_T^5}{\sum_{f=t,b} A_q^h(\tau_f)}, \quad (3.9)$$

where $\tau_f \equiv 4m_f^2/m_h^2$. This expression is valid for both models, since we did not modify the quark sector in the MCHM₅₊₁₀ with respect to the MCHM₅. The first term in the numerator takes into account the change in the $h\bar{f}f$ vertices appearing in the triangle loop, where we kept the contributions from the top and the bottom quark (see upper-left diagram of Figure 1 for $f = t$). The corresponding loop function $A_q^h(\tau_f)$ approaches 1 for $\tau_f \rightarrow \infty$ (which is already a good approximation for $\tau_t \approx 7.5$, leading to $A_q^h(\tau_t) \approx 1.03$) and vanishes proportional to τ_f for $\tau_f \rightarrow 0$. Its analytic form is given in Appendix A. We again consider only third generation fermions as the couplings of the others to the Higgs boson are strongly suppressed. The second term in the numerator of (3.9) represents the contribution arising from the virtual exchange of the heavy vector quarks (the top custodians), contained in Ψ^{T5} , which have significant couplings to the Higgs, see the second diagram in Figure 1. Remember that these resonances all couple diagonal to the gluons. Introducing already the corresponding lepton quantities which do not enter (3.9), but will be needed later, one obtains

$$\nu_F^5 = \begin{cases} v \sum_{n=2}^3 \frac{\text{Re}[(g_{h5}^F)_{nn}]}{m_{F_{n-1}}}, & F = T, E \\ 0, & F = Y \end{cases}, \quad (3.10)$$

$$\nu_F^{5+10} = \begin{cases} v \sum_{n=2}^4 \frac{\text{Re}[(g_{h10}^F)_{nn}]}{m_{F_{n-1}}}, & F = E \\ v \sum_{n=1}^3 \frac{\text{Re}[(g_{h10}^F)_{nn}]}{m_{F_n}}, & F = Y \end{cases}. \quad (3.11)$$

Note that since all the new resonances are much heavier than the Higgs boson, the loop functions that would multiply the above quantities are equal to 1 to excellent approximation and thus could be omitted.

For the effective coupling to photons we obtain

$$\kappa_\gamma^m = \frac{\sum_{f=t,b} N_c Q_f^2 \kappa_f^m A_q^h(\tau_f) + Q_\tau^2 \kappa_\tau^m A_q^h(\tau_\tau) + A_W^h(\tau_W) + N_c Q_t^2 \nu_T^5 + \sum_{F=E,Y} Q_F^2 \nu_F^m}{\sum_{i=t,b} N_c Q_i^2 A_q^h(\tau_i) + Q_\tau^2 A_q^h(\tau_\tau) + A_W^h(\tau_W)}, \quad (3.12)$$

where $N_c = 3$, $Q_t = 2/3$, $Q_b = -1/3$, $Q_{\tau,E} = -1$, $Q_Y = -2$, and $\tau_W \equiv 4m_W^2/m_h^2$. Here, we have already employed that $\kappa_W^{5,5+10} = 1$. The explicit expression for the form factor $A_W^h(\tau_W)$, encoding the W^\pm -boson contribution, can be found in Appendix A. The other quantities entering (3.12) have already been given before, see (3.4), (3.5), (3.10) and (3.11). The first, second, and third terms in the numerator above describe the effects of virtual SM-type quark, lepton, and W^\pm -boson exchange, respectively. The fourth and fifth term, on the other hand, correspond to the contributions of the custodians. Examples for corresponding one-loop graphs are shown in the second row of Figure 1. Note that the amplitude proportional to $A_W^h(\tau_W) \approx -6.25$ dominates in the SM and interferes destructively with the fermion contribution $A_q^h(\tau_f)$. Thus, adding just SM-like fermions, like a chiral t' , will reduce the effective coupling to photons. However, if the new fermions get part of their masses from another mechanism than the Higgs, like vector-like quarks or leptons, it is in principle possible to enhance κ_γ^m . We will see, that this is indeed the case for the MCHM₅₊₁₀.

3.2 Explicit Results in the Models at Hand

We now give the explicit predictions for the various quantities defined in the previous section for both the MCHM₅ and the MCHM₅₊₁₀. To that extend, we should also specify the values we use for the free parameters of the models, which we will do further below.

3.2.1 MCHM₅

Let us start with analyzing the MCHM₅, where we obtained easy analytic formulas for the masses and Higgs couplings in Section 2.1. Employing (2.12) we directly arrive at

$$\kappa_\tau^5 = (c_R^\tau)^2, \quad (3.13)$$

$$\kappa_t^5 = (c_R^t)^2, \quad (3.14)$$

while

$$\kappa_b^5 = 1. \quad (3.15)$$

The Higgs couplings to two τ leptons and two top quarks are thus predicted to be reduced in the MCHM₅. Note that at this point $c_R^{\tau,t}$ are free parameters of the model and thus allowed to take any value in their range of definition $0 \leq c_R^{\tau,t} \leq 1$. Physically, these parameters describe the mixings of the t_R and the τ_R to the new physics, which can reach from the decoupling limit $c_R^{\tau,t} \rightarrow 1$ up to a $O(1)$ mixing, which would start at $c_R^{\tau,t} \sim 1/\sqrt{2}$. For smaller values of $c_R^{\tau,t}$, the τ and the top quark will have typically stronger couplings with the new physics than the generic couplings (vector like masses) within the new physics sector. From the perspective of a composite Higgs model, $c_R^{\tau,t} \leq 1/\sqrt{2}$ would correspond

to a full compositeness, which should be kept in mind when studying the impact on Higgs decays. In that context, note that for $M \gg m_h$, which we will assume in the following, the predictions in Higgs physics are in principle independent of the vector-like mass M itself. However, if direct searches push M beyond the TeV range (see (2.8)), the scale of the absolute mass-mixing between elementaries and composites that is needed for $c_R^{\tau,t} \ll 1$ could become problematic.⁷

For the quantities related to the couplings of the heavy resonances, see (3.10), we obtain again from (2.12)

$$\nu_E^5 = (s_R^\tau)^2, \quad (3.16)$$

$$\nu_T^5 = (s_R^t)^2. \quad (3.17)$$

Combining these results, we arrive at

$$\kappa_g^5 \approx \frac{(c_R^t)^2 + A_q^h(\tau_b) + (s_R^t)^2}{1 + A_q^h(\tau_b)} = 1, \quad (3.18)$$

where we have used $A_q^h(\tau_t) \approx 1$. Thus, neglecting small deviations from this approximation, the production cross section for the Higgs boson in gluon-gluon fusion is unchanged in the MCHM₅, if one considers the low energy model of this work. There is a cancellation between corrections to the top Yukawa coupling and the contributions of the new top resonances, leading to a total contribution (normalized to the SM) of $(c_R^t)^2 + (s_R^t)^2 = 1$, which is independent of the parameters of the fermion sector. This result agrees with the findings of [71] (see also [72, 73]), which considers a complete composite Higgs model and thus additionally takes into account effects of the non-linearity of the Higgs sector, which are suppressed by v^2/f^2 . For the effective coupling of the Higgs to two photons we obtain in the same way

$$\begin{aligned} \kappa_\gamma^5 &= \frac{N_c(Q_t^2(c_R^t)^2 + Q_b^2 A_q^h(\tau_b)) + Q_\tau^2(c_R^\tau)^2 A_q^h(\tau_\tau) + A_W^h(\tau_W) + N_c Q_t^2 (s_R^t)^2 + Q_\tau^2 (s_R^\tau)^2}{N_c(Q_t^2 + Q_b^2 A_q^h(\tau_b)) + Q_\tau^2 A_q^h(\tau_\tau) + A_W^h(\tau_W)} \\ &= \frac{N_c(Q_t^2 + Q_b^2 A_q^h(\tau_b)) + Q_\tau^2((c_R^\tau)^2 A_q^h(\tau_\tau) + (s_R^\tau)^2) + A_W^h(\tau_W)}{N_c(Q_t^2 + Q_b^2 A_q^h(\tau_b)) + Q_\tau^2 A_q^h(\tau_\tau) + A_W^h(\tau_W)}. \end{aligned} \quad (3.19)$$

From the second line above, one can clearly see that due to the contribution of the new leptons, the structure that lead to $\kappa_g^5 \approx 1$ (or $\kappa_g^5 \approx (1 - 2v^2/f^2)/\sqrt{1 - v^2/f^2}$ in full composite models, see Section 3.4) for the Higgs coupling to two gluons is broken in κ_γ^5 .

⁷Note that in the full 5D/composite Higgs models there is a correlation between the elementary-composite mixing and the mass of the light custodians. However, in the lepton sector the direct bounds for current luminosities are weak, see e.g. [64], and do not affect significantly the parameter space. Regarding the quark sector, the latest and most stringent direct production bounds on the masses of vector-like quarks not coupling to the light generations are about ~ 700 GeV [70], however assuming a Higgs with SM couplings to fermions and gauge bosons. Anyway, all observables studied in the following are to excellent approximation independent of this parameter, due to a cancellation of the contributions of the top resonances and the SM-like top quark, see below. The only exception is the tree-level $ht\bar{t}$ coupling, which could be more constrained, due to the direct bound, leading to a reduced effect in $h \rightarrow b\bar{b}$ via tth production, see Figure 5.

Taking into account the lepton sector introduces a pattern which has not been considered in [71], namely a light particle ($m_\tau \ll m_h$) with a significant composite component (due to the mechanism which generates the light custodians). Because of $|A_q^h(\tau_\tau)| \approx 0.02 \ll 1$, the contributions of the SM-type lepton and the corresponding heavy resonances do not add up to a result which is independent from the model parameters. Their effect does *not* cancel, which is a very interesting and distinct feature of the lepton sector in these composite Higgs models.

Moreover, neglecting the tiny contribution proportional to $A_q^h(\tau_\tau)$, we can easily see that

$$\kappa_\gamma^5 \approx \frac{-5 + (s_R^\tau)^2}{-5}. \quad (3.20)$$

Thus, using the fact that $0 < (s_R^\tau)^2 < 1$ in the MCHM₅, we arrive at the clear prediction $\kappa_\gamma^5 < 1$. Physically, this is due to the fact that the new vector-like lepton adds a positive contribution to the numerator of (3.19), interfering destructively with the leading term proportional to $A_W^h(\tau_W)$. Note that, if we want to think of a complete GHU model producing our setup, we are missing 4 (6) heavier vector-like resonances of the first KK level in the T,E (B) sector which couple to the Higgs boson and could potentially enter the low energy predictions. However, we have seen that the light top-like modes present in our setup already contribute a structure $\sim (c_R^t)^2 + (s_R^t)^2 = 1$ to $\kappa_{g,\gamma}^5$, independent of the fermion parameters, and similar, but featuring different loop functions, for the τ . This agrees with the result of the corresponding full model, see [71, 72] (neglecting v/f corrections due to the modification of the Higgs sector for the moment). Thus the full fermion structure of the 5D model is present in our simplified low energy setup of light custodians, parametrized by c_R and s_R [65] (if one wants to consider the setup as an effective theory of a composite model). For the B sector, an analogous discussion holds, since neglecting v/f corrections, the predictions are unchanged with respect to the SM in our setup. Concerning potential contributions of resonances belonging to the first two generations, keep in mind that in GHU the total changes in Higgs physics due to light generations is negligible [71]. We will comment on further corrections to the above picture in full GHU models later on.

To summarize the findings of this section, the Higgs-production cross section is unchanged in our MCHM₅ setup in the gluon-gluon fusion, VBF and associated W^\pm -production channels to very good approximation, see (3.1)-(3.3) and (3.18), whereas it is reduced in associated top-quark pair production, see (3.6) and (3.14). As discussed above, the decay cross sections into photons, τ leptons and top quarks are reduced in the model. The explicit results for the production cross section times branching fraction in the different channels will be discussed in detail in Section 3.3.

3.2.2 MCHM₅₊₁₀

We now move over to the case of the MCHM₅₊₁₀. Here, naively it seems that one would have to resort completely to numerical methods to diagonalize the more complicated mass matrices (2.16) to finally obtain the Higgs couplings in the mass basis (2.20) that enter the various effective couplings. However, we can use a trick to avoid this procedure. First,

note that, neglecting the loop functions, (3.12) contains the structure

$$\lambda_F \equiv \begin{cases} \kappa_\tau^{5+10} + \nu_F^{5+10} = v \sum_{n=1}^4 \frac{\text{Re}[(g_{h10}^F)_{nn}]}{m_{F_{n-1}}}, & F = E \\ \nu_F^{5+10} = v \sum_{n=1}^3 \frac{\text{Re}[(g_{h10}^F)_{nn}]}{m_{F_n}}, & F = Y \end{cases}, \quad (3.21)$$

where, $m_{E_0} = m_\tau$. It turns out that these expressions can be summed analytically in closed form by using the relation (see e.g. [71])

$$\sum_n \frac{(g_{h10}^F)_{nn}}{\bar{m}_{F_n}} = \frac{\partial \log(\det \mathcal{M}_F)}{\partial v}, \quad (3.22)$$

where \bar{m}_{F_n} denote the mass eigenvalues belonging to the mass matrix \mathcal{M}_F , *i.e.* $\bar{m}_{F_n} = m_{F_{n-1}}$ for $F = E$ and $\bar{m}_{F_n} = m_{F_n}$ for $F = Y$. Note that in order to evaluate the right hand side of (3.22) one does not have to go to the mass basis. This allows us directly to also arrive at analytical expressions for the MCHM₅₊₁₀. Applying (3.22) to (2.16) we obtain⁸

$$\begin{aligned} \frac{\partial \log(\det \mathcal{M}_E)}{\partial v} &= \frac{1}{v} \frac{3v^2 \bar{y}\bar{y}\hat{y} + yM\tilde{M} - 3v^2 \bar{y}y'\tilde{y}}{v^2 \bar{y}\bar{y}\hat{y} + yM\tilde{M} - v^2 \bar{y}y'\tilde{y}} \\ &= \frac{1}{v} \left(1 + 2v^2 \frac{\bar{y}\hat{y}}{M\tilde{M}} - 2v^2 \frac{\tilde{y}\bar{y}y'}{yM\tilde{M}} + \mathcal{O}(\epsilon^3) \right), \end{aligned} \quad (3.23)$$

$$\frac{\partial \log(\det \mathcal{M}_Y)}{\partial v} = \frac{1}{v} \frac{4v^2 \bar{y}\hat{y}}{M\tilde{M} + 2v^2 \bar{y}\hat{y}} = \frac{1}{v} \left(4v^2 \frac{\bar{y}\hat{y}}{M\tilde{M}} + \mathcal{O}(\epsilon^3) \right), \quad (3.24)$$

where we have denoted $\epsilon \sim v/M, v/\tilde{M}$. Note that, for a sector that involves only heavy particles, *i.e.*, $F = Y$ (where $m_{Y_i} \gg m_h$ leads to $A_q^h(\tau) \approx 1$) the structure λ_Y (3.21) can directly be found in (3.12).

The structure leading to the expression (3.23) is however broken since the corresponding sector involves light SM-fermions, with a different loop function. It is nevertheless possible to extract the light-mode contribution from the corresponding equations to order ϵ^2 through the dimension six effective Lagrangian obtained from the integration of the corresponding vector-like fermions. Following [74] we obtain

$$v \frac{(g_{h10}^E)_{11}}{m_{E_0}} = 1 - v^2 \left(\frac{|\tilde{y}|^2}{2\tilde{M}^2} + \frac{|y'|^2}{M^2} + 2 \frac{\tilde{y}\bar{y}y'}{yM\tilde{M}} \right) + \mathcal{O}(\epsilon^3), \quad (3.25)$$

$$v \sum_{n=2}^4 \frac{(g_{h10}^E)_{nn}}{m_{E_{n-1}}} = v^2 \left(\frac{|y|^2}{2\tilde{M}^2} + \frac{|y'|^2}{M^2} + 2 \frac{\bar{y}\hat{y}}{M\tilde{M}} \right) + \mathcal{O}(\epsilon^3). \quad (3.26)$$

In this approximation it is thus possible to use (3.22)-(3.26) to sum up the different contributions to κ_γ^{5+10} in closed form to analytical results, see (3.5), (3.11), and (3.12). At this point some comments are in order.

⁸In the same way we could have derived the corresponding expressions for the MCHM₅, getting the same results as the ones obtained employing the mass basis.

Parameter	central value [GeV]
$ m \approx -\tilde{m} $	1
$ m' \approx -\tilde{m}' $	100
$ \tilde{m} $	100
M	400
\tilde{M}	450

Table 1. Assumptions for the free parameters of the MCHM₅₊₁₀, defining $m = v/\sqrt{2}y$ for the various Yukawa couplings. All values are varied around the central value m_{cent} in the range $[0.4, 2.5]m_{\text{cent}}$. Moreover, besides the vector-like mass terms M and \tilde{M} , all parameters are allowed to have arbitrary phases.

The expressions above contain quite a number of parameters and so will κ_i^{5+10} , $i = \tau, \gamma$. In order to make transparent the predictions of the MCHM₅₊₁₀, we should specify the assumptions we make on the parameters and visualize the predictions for the different quantities entering the effective Higgs couplings. To that extend we scan over the parameter-space of the model, varying the mass parameters in the range $[0.4, 2.5]m_{\text{cent}}$ around their central values m_{cent} , which are given in Table 1, with a flat distribution (for the various Yukawa couplings we define $m = v/\sqrt{2}y$). Note that all parameters, besides the vector-like mass terms M and \tilde{M} are allowed to have arbitrary phases. The magnitude of the corresponding parameters is motivated by the assumption that only the τ_R , responsible for the relatively large mass of the τ , couples significantly to the new physics. As discussed, this corresponds for example to the low energy tail of composite models/GHU models featuring an A_4 symmetry, and matches well with phenomenological constraints. The chosen range for the (Kaluza-Klein) masses of the light resonances $160 \text{ GeV} < M, \tilde{M} < 1125 \text{ GeV}$ corresponds to the natural range of models addressing the gauge hierarchy problem. The parameters will be constrained to result in a mass for the τ lepton that is in agreement with the experimental value, evaluated at the scale of the new resonances. As it turns out that the τ_R has a similar degree of compositeness as its light custodian partners (with opposite “sign”), we assume that $\tilde{m} = -m(1 \pm 10\%)$ and $\tilde{m}' = -m'(1 \pm 10\%)$. This approximate equality has important implications on the structure of (3.23), which then becomes $\partial \log(\det \mathcal{M}_E)/\partial v \approx 1/v$. Thus, as in the case of the MCHM₅, there is a cancellation between the correction to the SM τ Yukawa and the heavy resonances entering κ_γ^m , that would lead to the same contribution of the complete τ sector as the τ contribution in the SM, *i.e.* a cancellation of the new physics effects *if* the τ was heavier than the Higgs boson. However, as for the MCHM₅, this is broken completely by the different loop functions for the τ and its custodian partners. Nevertheless, this structure assures that, like in the MCHM₅, we also capture the whole physics of the complete KK tower, if we want to consider our setup as a low energy tail of a GHU model.⁹ In contrast to the

⁹Note that the structure leading to $\partial \log(\det \mathcal{M}_E)/\partial v \approx 1/v$ grasps the physics of the whole KK tower even in the case of the MCHM₅₊₁₀, where due to the various fermion representations present in the model two different trigonometric functions can arise [72]. This is due to the fact that the more composite τ_R just can mix with the **10**, being only the almost elementary SM doublet l_L who connects both sectors. Therefore,

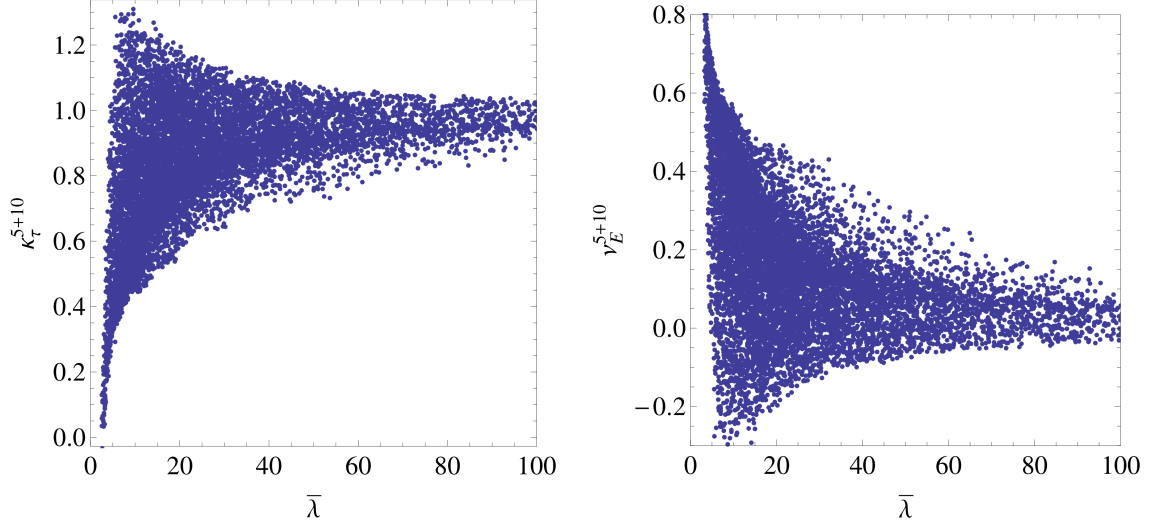


Figure 2. Predictions for the quantities κ_τ^{5+10} and ν_E^{5+10} in the MCHM_{5+10} plotted versus the parameter $\bar{\lambda} = 2M\tilde{M}/(v^2|y'\bar{y}|)$, measuring the vector-like masses over the product of the compositeness of the right handed τ with the Yukawa couplings of the new resonances. The points correspond to a scan over the parameter-space of the model. See text for details.

case of the MCHM_5 , there are now additional contributions from exotic $Q = -2$ fermions Y . In this case, as mentioned before, we do consider a complete KK level, as the missing heavy Y -fields belong to fundamental representations of $SO(5)$ and thus have negligible Higgs-couplings.

We thus expect in principle quite different signatures in Higgs Physics in the MCHM_{5+10} with respect to the MCHM_5 . Putting more SM-leptons or the quarks into a **10** of $SO(5)$ would spoil the above considerations and thus the model we consider is a conservative choice, if one wants to capture the full structure of a composite model via the light-particle spectrum. While we expect the numerical results to change once we put the whole third generation into a **10**, the *qualitative* behavior is expected nevertheless to be similar to our setup [65] and thus the model can be seen as a simple setup that allows to understand the behavior of the lepton sector of the full MCHM_{10} .

In order to explore the new features of the MCHM_{5+10} we now show scatter plots representing the predictions for κ_τ^{5+10} , $\nu_{E,Y}^{5+10}$, and λ_E for 10000 parameter points. They have all been obtained by an exact numerical diagonalization of the mass matrices (2.16) and a subsequent numerical evaluation of the Higgs couplings in the mass basis (2.20), employing the parameters given in Table 1, which are varied as described before. We plot the results with respect to the parameter

$$\bar{\lambda} = \frac{2M\tilde{M}}{v^2|y'\bar{y}|}, \quad (3.27)$$

similarly to what happens in the model considered in Appendix B of [72], the breaking of the above pattern in the complete composite model will be governed by the magnitude of $\lambda_l^{(10)}$, a small parameter controlled by the size of the tau mass over the τ_R linear coupling.

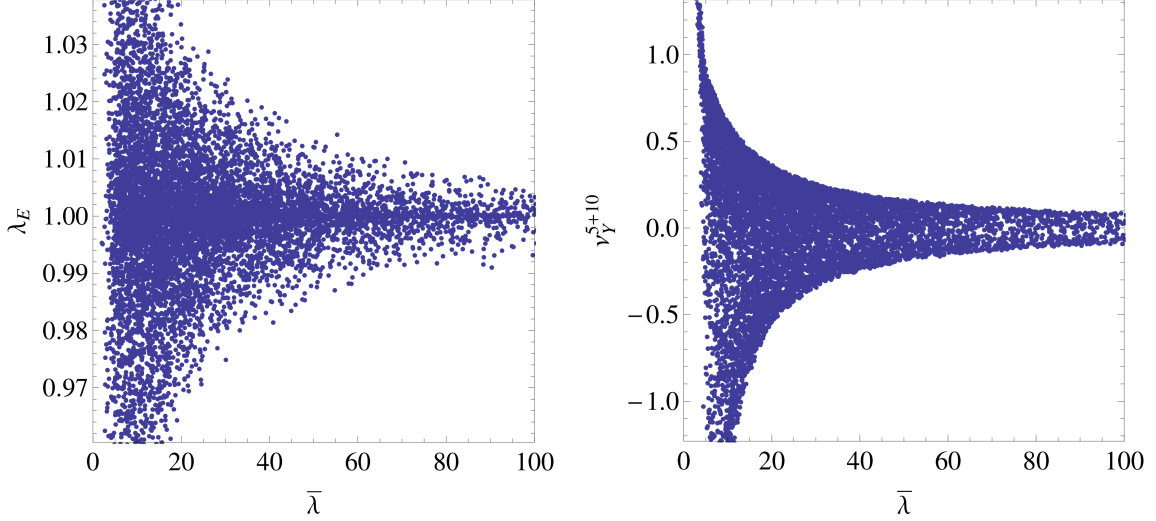


Figure 3. Predictions for λ_E and ν_Y^{5+10} in the MCHM₅₊₁₀ plotted versus $\bar{\lambda}$, measuring the scale of the vector-like masses of the new resonances over their Yukawa couplings. The points correspond to a scan over the parameter-space of the model. See text for details.

which measures the vector-like masses over the compositeness of the right handed τ times the scale of the Yukawa couplings of the new resonances. Note that, due to $y' \approx -\hat{y}$, at the same time it also is a measure for the size of the vector-like masses over the scale of the Yukawa couplings of the new resonances alone. It is thus expected that all the physical predictions of the model should scale with this parameter.

In Figure 2 we show the effective coupling κ_τ^{5+10} as well as ν_E^{5+10} in the MCHM₅₊₁₀ with respect to $\bar{\lambda}$. One can clearly see that also in the MCHM₅₊₁₀ the couplings of the τ lepton to the Higgs boson are generically reduced. They are mostly in the range $0 < \kappa_\tau^{5+10} < 1$, as for the MCHM₅ (see (3.13)), however a small enhancement seems also possible. For a squared compositeness scale of roughly one order of magnitude below the squared scale of the light resonances, $\bar{\lambda} \sim 10$, one can have a depletion of up to $\kappa_\tau^{5+10} \sim 0.5$. In the decoupling regime of large $\bar{\lambda}$, one approaches the SM value of $\kappa_\tau = 1$, as expected. The contributions of the resonances of the τ sector also become important for low $\bar{\lambda}$, *i.e.* of the order $\nu_E^{5+10} \sim 0.5$ for $\bar{\lambda} \sim 10$ (for the region with the largest density of scatter points), as can be read off from the right plot in the figure. From the plots one can already suspect the numerical confirmation of the discussion below (3.24), *i.e.*, that in the MCHM₅₊₁₀, in analogy to the MCHM₅, the relation $\lambda_E = \kappa_\tau^{5+10} + \nu_E^{5+10} = 1$ holds to good approximation. This can be seen more clearly in the left panel of Figure 3, where we plot λ_E versus $\bar{\lambda}$ and find that indeed $\lambda_E \approx 1$. The breaking of the exact relation is due to the fact that we did allow for small variations $\tilde{m} = -m(1 \pm 10\%)$ and $\hat{m} = -m'(1 \pm 10\%)$. Remember however, that both contributions to λ_E enter κ_γ^{5+10} with a different loop function. In the right panel of Figure 3 we show our predictions for ν_Y^{5+10} , plotted again versus $\bar{\lambda}$. We can see that this contribution can become negative which allows for a constructive interference with the W^\pm -loop in $h \rightarrow \gamma\gamma$ and finally leads to a possible enhancement in the Higgs decay into

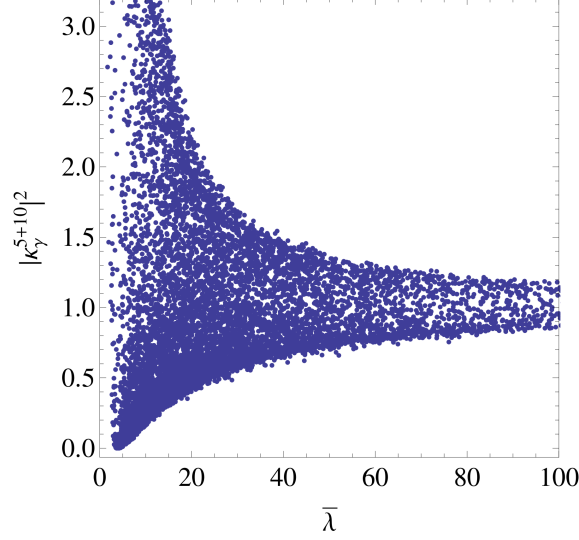


Figure 4. Predictions for $|\kappa_\gamma^{5+10}|^2$ plotted versus $\bar{\lambda}$. Note that the dependence on the parameters of the quark sector drops out to good approximation. The points correspond to a scan over the parameter-space of the model. See text for details.

two photons, which is not possible to get in the MCHM₅.

Finally, we come to the results for κ_γ^{5+10} , which due to the fact that the quark sector is unchanged with respect to the MCHM₅ takes the explicit form

$$\kappa_\gamma^{5+10} \approx \frac{N_c(Q_t^2 + Q_b^2 A_q^h(\tau_b)) + A_W^h(\tau_W) + Q_\tau^2(\kappa_\tau^{5+10} A_q^h(\tau_\tau) + \nu_E^{5+10}) + Q_Y^2 \nu_Y^{5+10}}{N_c(Q_t^2 + Q_b^2 A_q^h(\tau_b)) + A_W^h(\tau_W) + Q_\tau^2 A_q^h(\tau_\tau)}. \quad (3.28)$$

The fact that, as explained before, $|\kappa_\gamma^{5+10}|^2$ can now become bigger than one via the potentially negative contributions due to ν_Y^{5+10} can be seen clearly from the plot in Figure 4. We discover that for $\bar{\lambda} \sim 20$ we can get up to a doubling in the decay cross section $h \rightarrow \gamma\gamma$. Note however, that from the UV perspective of a GHU model, there are further constraints on the parameters. We will elaborate on this below.

3.3 Phenomenological Implications

We finally arrive at the predictions of the models for the various Higgs channels studied at the LHC. In the following, we are interested in the predictions for the Higgs-production cross sections times branching ratios in the models at hand, normalized to the corresponding SM expectations

$$R_f^m \equiv \frac{[\sigma(pp \rightarrow h)\text{Br}(h \rightarrow ff)]_{\text{MCHM}_m}}{[\sigma(pp \rightarrow h)\text{Br}(h \rightarrow ff)]_{\text{SM}}}, \quad (3.29)$$

for $f = \gamma, \tau, b, W, Z$, where $m = 5, 5+10$. Moreover, we will also look at processes initiated by an explicit production mechanism of the Higgs Boson

$$R_f^{i;m} \equiv \frac{[\sigma(i)\text{Br}(h \rightarrow ff)]_{\text{MCHM}_m}}{[\sigma(i)\text{Br}(h \rightarrow ff)]_{\text{SM}}}, \quad (3.30)$$

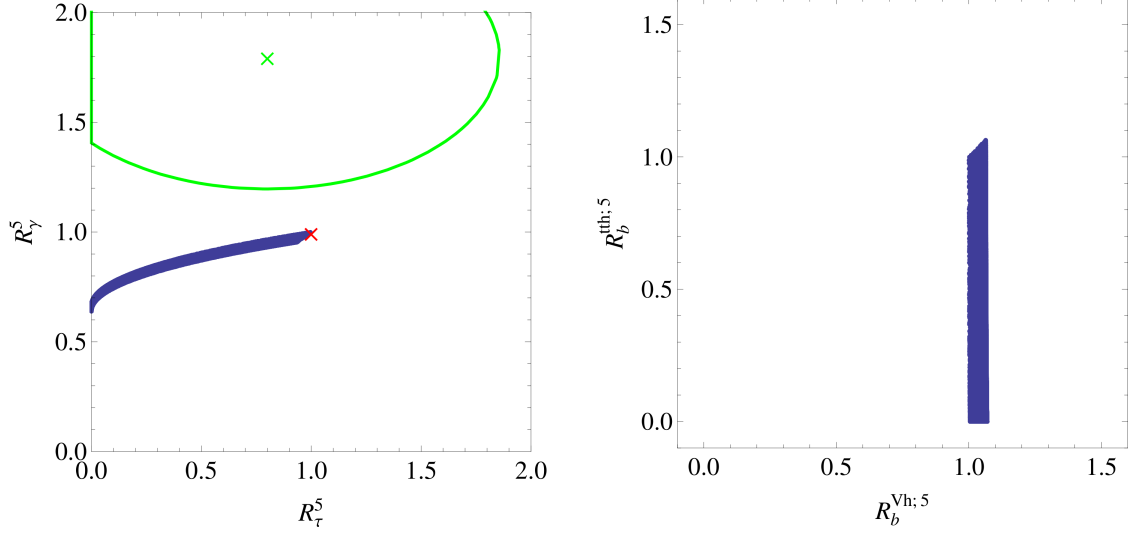


Figure 5. Left: Prediction for the production cross section times branching fraction for $pp \rightarrow h \rightarrow \gamma\gamma$ in the MCHM₅ relative to the SM versus the same ratio for $pp \rightarrow h \rightarrow \tau\tau$. The experimental 1σ contour from ATLAS is indicated as a green line (neglecting possible correlations). The best fit value $(R_\gamma, R_\tau)_{\text{exp}} \approx (1.8, 0.8)$ is shown as a green cross and the SM prediction $(R_\gamma, R_\tau)_{\text{SM}} = (1, 1)$ as a red cross. Right: Higgs production cross section in the tth channel times branching fraction $h \rightarrow b\bar{b}$ in the MCHM₅ relative to the SM vs the equivalent ratio, assuming that the Higgs Boson has been produced via associated vector-boson production.

$i = gg \rightarrow h, \text{ VBF}, Vh, tth$. For converting the results for the Higgs decays, derived in Section 3, into branching fractions, one has to take into account also the change in the total decay rate $\Gamma(h)$ of the Higgs boson. For a SM Higgs with mass $m_h \approx 125 \text{ GeV}$, the total rate is dominated by its decay into bottom quarks. Explicitly, one finds $\text{Br}(h \rightarrow b\bar{b}) \approx 0.59$, $\text{Br}(h \rightarrow WW) \approx 0.23$, $\text{Br}(h \rightarrow gg) \approx 0.07$, $\text{Br}(h \rightarrow \tau\tau) \approx 0.06$, and $\text{Br}(h \rightarrow ZZ) \approx 0.03$. In consequence, for the models at hand we arrive at

$$R_\Gamma^m \equiv \frac{\Gamma(h)_{\text{MCHM}_m}}{\Gamma(h)_{\text{SM}}} \approx 0.59 [\kappa_b^m]^2 + 0.07 |\kappa_g^m|^2 + 0.06 [\kappa_\tau^m]^2 + 0.28. \quad (3.31)$$

The sought ratio of the branching fractions can now be obtained as

$$\frac{\text{Br}(h \rightarrow ff)_{\text{MCHM}_m}}{\text{Br}(h \rightarrow ff)_{\text{SM}}} = \frac{\Gamma(h \rightarrow ff)_{\text{MCHM}_m}}{\Gamma(h \rightarrow ff)_{\text{SM}}} / R_\Gamma^m. \quad (3.32)$$

It turns out, that the changes in the decay rate for the models considered will be of minor importance since we have $\kappa_b^5 = \kappa_b^{5+10} \approx \kappa_g^5 = \kappa_g^{5+10} \approx 1$. We will nevertheless take them into account in the numerical analysis.

We start with the results for the setup corresponding to the MCHM₅. In the left panel of Figure 5 we show the predictions for the change of the important discovery channel $pp \rightarrow h \rightarrow \gamma\gamma$ relative to the SM (neglecting for the moment tth production)

$$R_\gamma^5 \approx \frac{[\text{Br}(h \rightarrow \gamma\gamma)]_{\text{MCHM}_5}}{[\text{Br}(h \rightarrow \gamma\gamma)]_{\text{SM}}}, \quad (3.33)$$

versus the change in the channel $pp \rightarrow h \rightarrow \tau\tau$

$$R_\tau^5 \approx \frac{[\text{Br}(h \rightarrow \tau\tau)]_{\text{MCHM}_5}}{[\text{Br}(h \rightarrow \tau\tau)]_{\text{SM}}}. \quad (3.34)$$

Here, we have already employed the results $\sigma(\text{VBF})_{\text{MCHM}_m} = \sigma(\text{VBF})_{\text{SM}}$ and $\sigma(Vh)_{\text{MCHM}_m} = \sigma(Vh)_{\text{SM}}$, see (3.2) and (3.3). Moreover, due to $\kappa_g^5 = \kappa_g^{5+10} \approx 1$, we also could use $\sigma(gg \rightarrow h)_{\text{MCHM}_m} \approx \sigma(gg \rightarrow h)_{\text{SM}}$, see (3.1). To obtain the predictions shown in the plots, we have used the results derived from evaluating (3.1), (3.7), (3.31), and (3.32). We show the full range for $0 \leq c_R^{\tau,t} \leq 1$. For illustration, we give the experimental 1σ contour from ATLAS, extracted from [3], as a green line (neglecting possible correlations), whereas the best fit value $(R_\gamma, R_\tau)_{\text{exp}} \approx (1.8, 0.8)$ is shown as a green cross. The results are comparable to those of the CMS experiment. The SM prediction $(R_\gamma, R_\tau)_{\text{SM}} = (1, 1)$ is given as a red cross. Although it is still too early to derive too strong conclusions from the experimental situation, one can see that if the experimental errors shrink and the central values would remain in the same ballpark, the MCHM₅ would not be able to account for the resulting discrepancy. Going away from the SM limit (*i.e.* away from the decoupling limit $c_R \rightarrow 1$) leads to a stronger tension with experiment than in the SM due to the fact that in the MCHM₅ one can only get a reduction in the $\tau\tau$ channel together with a reduction in the $\gamma\gamma$ channel. The small width of the prediction for R_γ^5 , for constant R_τ^5 , reflects the fact that the corrections due to the quark sector are of minor importance in R_γ^5 , see (3.20). The strong correlation between R_γ^5 and R_τ^5 , both depending to good approximation only on the same parameter c_R^τ (see also below) allows to easily constrain or rule out the model, after experimental results become more precise.

We now turn to the decay of the Higgs boson into two bottom quarks. Note that, due to $\kappa_b^5 = 1$ and $\sigma(Vh)_{\text{MCHM}_m} = \sigma(Vh)_{\text{SM}}$, the process $q\bar{q}^{(\prime)} \rightarrow V^* \rightarrow Vh$, $V = W, Z$, with a subsequent decay $h \rightarrow b\bar{b}$ remains SM-like to good approximation (the deviation of R_Γ^5 from 1 due to $\kappa_\tau^5 \neq 1$ is only at the level of a few per cent)

$$R_b^{Vh;5} \approx 1. \quad (3.35)$$

However, due to $\kappa_t^5 < 1$ the search channel $gg \rightarrow t\bar{t}^*t^*\bar{t} \rightarrow t\bar{t}h$, $h \rightarrow b\bar{b}$ can receive a sizable suppression, which is illustrated in the right panel of Figure 5, where we show $R_b^{tth;5}$ versus $R_b^{Vh;5}$. Once the experimental situation in these channels improves they will become a superb tool for measuring directly a possible reduction in the $t\bar{t}h$ coupling. This prediction of the MCHM₅, together with an expected more SM-like behavior in the Vh channel (both in tentative agreement with latest CMS results [4]), would allow for another possibility to test the model. Since the formulas in the MCHM₅ are easy enough, it is even possible to solve for the important parameters of the model, c_R^t and c_R^τ , in dependence on the $R_f^{(i);5}$. Using (3.6) and (3.30) we directly obtain the approximate relation

$$(c_R^t)^2 \approx \sqrt{R_b^{tth;5}}. \quad (3.36)$$

In the same way one can solve for c_R^τ , using the information from R_γ^5 and R_τ^5 . The approximate result, neglecting corrections due to $A_q^h(\tau_t) \neq 1$, $A_q^h(\tau_\tau) \neq 0$ and $R_\Gamma^5 \neq 1$, is

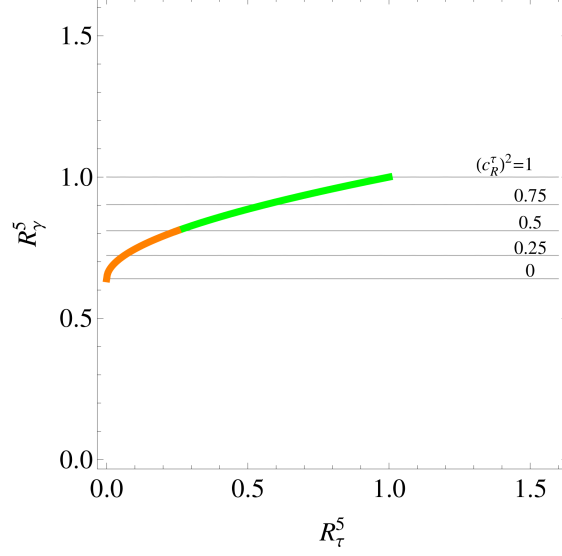


Figure 6. Left: Prediction for the production cross section times branching fraction for $pp \rightarrow h \rightarrow \gamma\gamma$ in the MCHM₅ relative to the SM versus the same ratio for $pp \rightarrow h \rightarrow \tau\tau$. The intersections with the horizontal lines indicate the parameter $(c_R^\tau)^2$ that results in the corresponding prediction in the (R_τ^5, R_γ^5) -plane. See text for details.

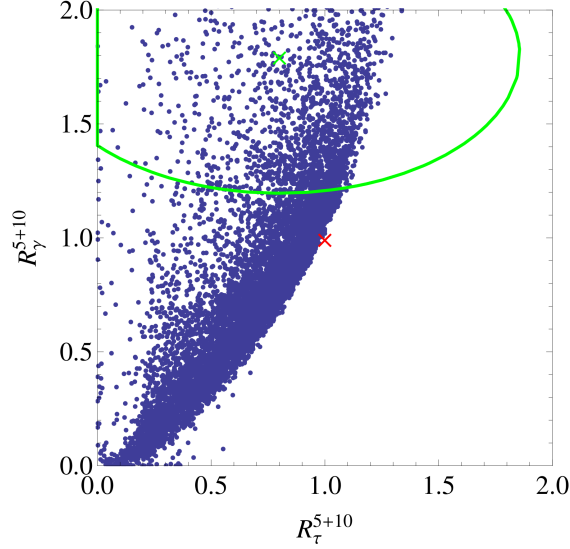


Figure 7. Production cross section times branching fraction for $pp \rightarrow h \rightarrow \gamma\gamma$ in the MCHM₅₊₁₀ relative to the SM versus the same ratio for $pp \rightarrow h \rightarrow \tau\tau$. The experimental 1σ contour from ATLAS is again given as a green line. The best fit value $(R_\gamma, R_\tau)_{\text{exp}} \approx (1.8, 0.8)$ is shown as a green cross and the SM prediction $(R_\gamma, R_\tau)_{\text{SM}} = (1, 1)$ as a red cross. The points correspond to a scan over the parameter-space of the model.

shown in Figure 6 for illustration. The intersection of the straight lines, corresponding to different c_R^τ , with the prediction in the (R_τ^5, R_γ^5) -plane, depicted by the colored line, gives

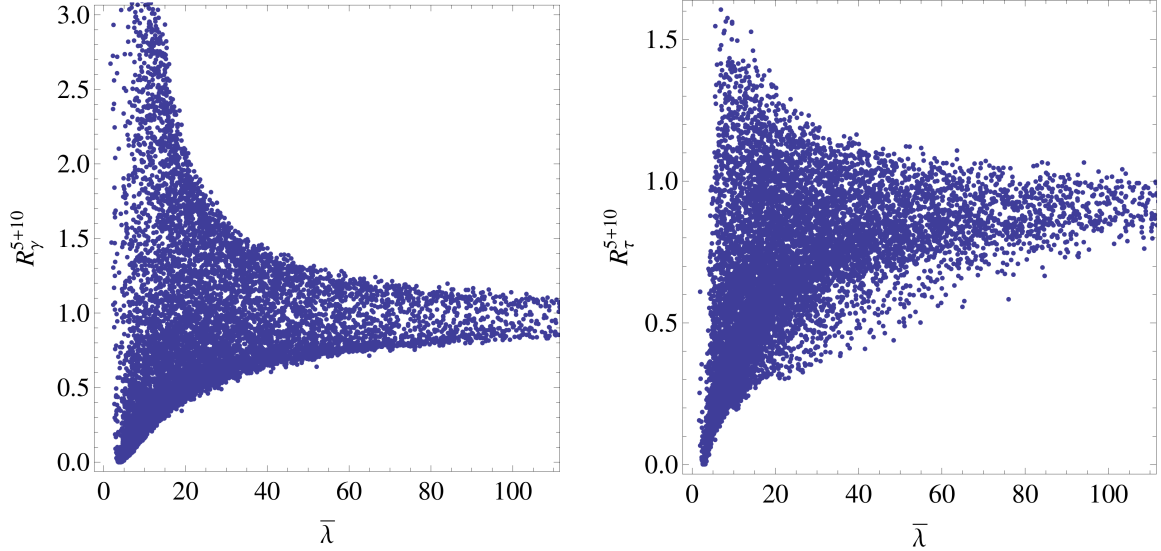


Figure 8. Left: Predictions for R_γ^{5+10} plotted versus the parameter $\bar{\lambda} = 2M\tilde{M}/(v^2|y'\bar{y}|)$, measuring the vector-like masses in the lepton sector over the product of the compositeness of the right handed τ with the Yukawa couplings of the new leptonic resonances. Right: Analogous plot, now for R_τ^{5+10} . The points correspond to a scan over the parameter-space of the model. See text for details.

the MCHM₅ result in dependence on the input parameter c_R^τ . This would allow to get insight about the possible parameters of the extended fermion sector, once a more precise measurement (compatible with the predictions of the model) would be established. The orange color indicates values of $c_R^\tau < 1/\sqrt{2}$ that correspond to a large compositeness of the order of $m' \sim M$ and should be taken with caution.

Finally, it is clear from the previous discussion that also, if the Higgs boson is produced in gluon-gluon fusion, VBF or associated W^\pm -production, the double-vector boson production through a Higgs remains unchanged to good approximation in the MCHM₅, see (3.8), which is in reasonable agreement with first measurements of the experiments [3, 4].

We now move to the discussion of the MCHM₅₊₁₀. As explained in Section 3.2.2, we expect different predictions for this version of the model. We start again by studying the correlation between R_γ^{5+10} and R_τ^{5+10} , which is depicted in the plot in Figure 7. Now, as detailed in Section 3.2.2, the decay into photons can receive an enhancement with respect to the SM. Moreover, also in the MCHM₅₊₁₀ one gets the rough prediction $R_\tau^{5+10} < 1$. Taken together this allows, in contrast to the MCHM₅, for the possibility to reach the best fit value $(R_\gamma, R_\tau)_{\text{exp}} \approx (1.8, 0.8)$ in the MCHM₅₊₁₀. Note that this is possible without spoiling the rough agreement with the SM in the other channels, which are (besides $t\bar{t}h$ production) unchanged to good approximation in the models at hand. Moreover, although due to the new $Q = -2$ resonances the correlations are not as strong as in the MCHM₅, still, finding e.g. a reduced $\gamma\gamma$ signal, together with an enhanced $\tau\tau$ rate, would exclude the model. To judge which scales for the parameters of the model lead to which prediction, we give in the left plot of Figure 8 our result for R_γ^{5+10} versus the parameter $\bar{\lambda}$ (see

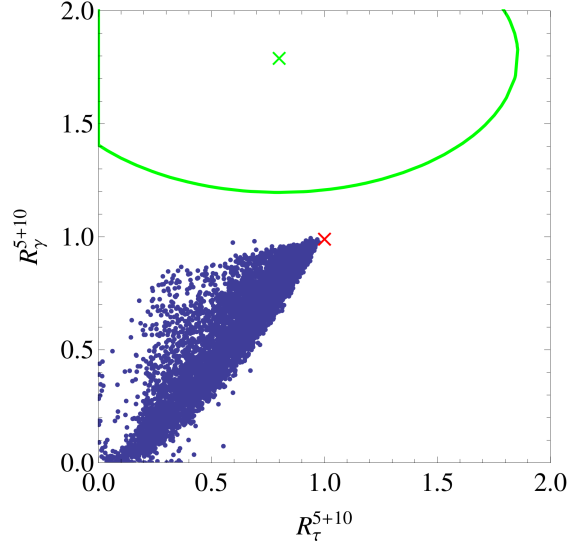


Figure 9. Production cross section times branching fraction for $pp \rightarrow h \rightarrow \gamma\gamma$ in the MCHM_{5+10} relative to the SM versus the same ratio for $pp \rightarrow h \rightarrow \tau\tau$. The experimental 1σ contour from ATLAS is again given as a green line. The best fit value $(R_\gamma, R_\tau)_{\text{exp}} \approx (1.8, 0.8)$ is shown as a green cross and the SM prediction $(R_\gamma, R_\tau)_{\text{SM}} = (1, 1)$ as a red cross. The points correspond to a scan over the parameter-space of the model with the constraint $\nu_Y^{5+10} > 0$ from GHU models.

(3.27)), measuring the vector-like masses over the product of the compositeness of the right handed τ with the Yukawa couplings of the new leptonic resonances. This parameter is still appropriate, as the impact of the new quark sector on R_γ^{5+10} is very limited. We deduce that for moderately low scales $\bar{\Lambda} \sim 20$, an enhancement of up to a factor of 2 in the $pp \rightarrow h \rightarrow \gamma\gamma$ channel is possible (see [6] in this context). We stress that, although significant changes in the couplings of the leptons to the Higgs sector appear, the agreement with electroweak precision observables is saved due to the custodial symmetry. In the right panel of the figure, we show the analogous plot for R_τ^{5+10} . We observe that a reduction $R_\tau^{5+10} < 0.5$ would correspond to scales $\bar{\Lambda} < 20$ (a non-negligible enhancement possible for such low scales comes with extremely large values of R_γ^{5+10}). Such low scales would still be viable, given that the vector-like masses themselves are not beyond the TeV scale. Note that also in the MCHM_{5+10} the mass eigenvalues of the resonances alone have only a limited impact on the size of the effects, as a larger mass can be compensated by larger Yukawa couplings. The question then becomes how large one could assume the values for the Yukawa couplings. For $\bar{\Lambda}$ of $\mathcal{O}(1)$, these Yukawas would be of the order of the masses of the heavy resonances over v which could become problematic. Finally, concerning the decay into bottom quarks, the predictions in the MCHM_{5+10} are comparable to those in the MCHM_5 , due to the unchanged quark sector.

We have seen that in the MCHM_{5+10} the strong correlations present in the MCHM_5 are washed out, making on the one-hand side the model less predictive but on the other allow in principle for a better agreement with preliminary results from the LHC. Still, as discussed above, correlations and empty regions of parameter space remain, allowing to

test the model.

So far, we have constrained the parameters of the model roughly from naturalness arguments and phenomenology. However, as already mentioned before, in GHU models there are more correlations present between the parameters. For example such correlations will lead to relations between the numerator and the denominator of $\bar{\lambda}$, making it not a completely free parameter anymore, and the same holds true for $c_R^{t,\tau}$. The results given above hence are more general in comparison to considering GHU models as a UV completion [65]. The predictions include those of GHU models as a subset. Moreover, it turns out that always $\nu_Y^{5+10} > 0$ in GHU, making the model more predictive with respect to R_γ^{5+10} . In Figures 9 and 10 we plot again the same quantities given before, now employing this condition.

First, we can see that the condition eliminates the small amount of points corresponding to $R_\tau^{5+10} > 1$. This can be also understood from (3.25) and (3.26). Implementing the information from the GHU model leads to $\text{Re}(\bar{y}\hat{y}) \approx -\text{Re}(\bar{y}y') > 0$ (see (3.24)) and thus, directly from (3.25) we get $\kappa_\tau^{5+10} < 1$. Moreover, all the parameter-space with $R_\gamma^{5+10} > 1$ is gone, as expected. In Figure 10 we give the dependence of the individual quantities on $\bar{\lambda}$ in the constrained setup for completeness. Seeing our MCHM₅₊₁₀ as the low energy limit of a GHU model thus leads again to the robust prediction of $R_\gamma^{5+10}, R_\tau^{5+10} < 1$. Exploring the (R_γ, R_τ) -plane experimentally can on the one hand give hints if an extended fermion sector featuring custodial protection, as studied in this work, could exist and on the other hand could also say something about the possible UV completion of such a sector.

Finally, as in the MCHM₅, due to the SM-like coupling of the Higgs boson to gauge bosons (and bottom quarks), the double-vector boson production through a Higgs also remains unchanged to good approximation if the Higgs boson is produced in gluon-gluon fusion, VBF or associated vector-boson production.

3.4 Impact of the Non-Linearity of the Higgs

Up to now, we have neglected the effects arising from the pseudo-Goldstone boson nature of the Higgs boson in the corresponding UV completions of our models. Considering this will lead to shifted Higgs couplings to the different fermions and gauge bosons of the spectrum. In the latter case, neglecting the mixing of the SM gauge bosons to their composite counterparts, everything is fixed by the quantum numbers and the symmetry breaking defining the composite model. For the models that we study we obtain [75]

$$\kappa_W^m = \kappa_Z^m = \cos\left(\frac{v}{f}\right) \approx \sqrt{1-\xi}, \quad m = 5, 5+10, \quad (3.37)$$

where we have defined $\xi = v^2/f^2$ as usual.

In the case of fermions, we have to make the difference between the two cases considered in this paper, since the explicit expressions for these additional corrections depend also on the different representations chosen for fermions. In the MCHM₅, the corresponding modifications of the Higgs couplings to SM fermions read

$$\kappa_f^5 \rightarrow \kappa_f^5 \cos\left(\frac{2v}{f}\right) / \cos\left(\frac{v}{f}\right) \approx \kappa_f^5(1-2\xi)/\sqrt{1-\xi}, \quad (3.38)$$

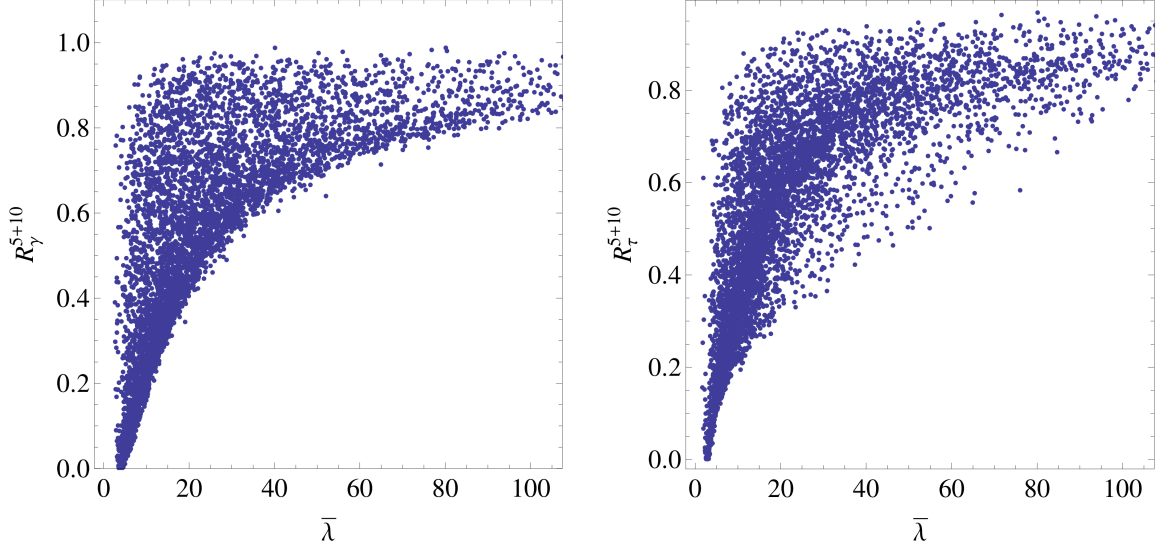


Figure 10. Left: Predictions for R_γ^{5+10} plotted versus the parameter $\bar{\lambda}$. Right: Analogous plot, now for R_τ^{5+10} . The points correspond to a scan over the parameter-space of the model, employing the constraint $\nu_Y^{5+10} > 0$ from GHU models. See text for details.

where f is running over all the fermions of the SM. Here and in the following we neglect v^2/f^2 corrections to contributions which are already suppressed by the new physics scale. In this approximation, all the ν_F^m factors remain unchanged. The previous shifts in the fermion couplings to the Higgs boson will lead also to a suppression of the effective coupling to gluons, which can be written as

$$\kappa_g^5 \approx \cos\left(\frac{2v}{f}\right) / \cos\left(\frac{v}{f}\right) \approx (1 - 2\xi)/\sqrt{1 - \xi}. \quad (3.39)$$

In the case of the MCHM_{5+10} the expressions have to take into account that the τ_R is living in a **10** while the opposite chirality is embedded in a fundamental representation of $SO(5)$. This leads to [72]

$$\kappa_\tau^{5+10} \rightarrow \kappa_\tau^{5+10} \cos\left(\frac{v}{f}\right) \approx \kappa_\tau^{5+10} \sqrt{1 - \xi} \quad (3.40)$$

while the other couplings change analogously as in the MCHM_5 . Finally, the change in κ_γ^m can be worked out for both models by applying the replacements given above to (3.12) (including the change in the Higgs coupling to W^\pm -bosons).

We have implemented all these additional corrections in our phenomenological study, employing $\xi = 0.2$, to see to what extent the previous picture is changed. The neglected effects arising from the non-linearity of the Higgs are a subleading correction to the shift in the Yukawa couplings for both the top quark and the τ lepton in the regime where both fermions are mostly composite and strongly interact with the different vector-like

resonances, although it can be important in the decoupling limit.¹⁰ Comparing the plot in the left panel of Figure 11 to the equivalent one shown before, see Figure 5, we can see that taking into account the pseudo-Goldstone character of the Higgs boson leads to a further reduction in both the $gg \rightarrow h \rightarrow \gamma\gamma$ and $\tau\tau$ channels in the MCHM₅, where for the latter the Higgs is assumed to be produced in VBF or Vh production. Even though this is not shown in the figure, the same holds for gluon-gluon fusion. The different trigonometric rescaling appearing for the τ in the MCHM₅₊₁₀, see (3.40), leads to modifications to this picture, as can be seen comparing the right panel of the previous figure to Figure 9. In this case, the larger suppression for the other fermions can in principle enhance $h \rightarrow \tau\tau$ through VBF and Vh production. This is not longer true if we consider other production mechanisms like $gg \rightarrow h$ or tth . A similar enhancement can happen in both models for $h \rightarrow \gamma\gamma$ in the production mechanisms induced by weak gauge bosons, as is shown in Figure 12, because the smaller trigonometric suppressions of the couplings of the latter still allow for an enhancement in the production cross section times branching fraction, despite the reduction in κ_γ^m due to the composite fermions. We should notice however that these plots are made using a moderately large value of $\xi = 0.2$, which has to be compared for instance with the one arising from a 5D construction with a small KK scale of 1.5 TeV, which is $\xi \approx 0.1$. Concerning the changes in Higgs decays to bottom quarks, the trigonometric rescalings of the fermion interactions lead to a reduction in both $R_b^{Vh;5}$ and the maximum possible $R_b^{tth;5}$. Finally, as can be seen from the red regions in the last two figures, which show the predictions neglecting the impact of light lepton custodians, their effect is important and should be taken into account.

4 Conclusions

We have studied the impact of modified fermion sectors, featuring a custodial symmetry that protects the $Zb_L b_L$ and $Z\tau_R \tau_R$ vertices, on Higgs production and decay. On the one hand, these setups can be thought of as simple extensions of the SM, viable on their own. On the other hand, they can be particularly motivated as the low energy tail of composite Higgs models (MCHM_{5,10}) or models of gauge-Higgs unification. Here the particles we consider arise as light custodians, associated to the significantly composite top quark and τ lepton. Due to the simple structure of the setups considered, we were able to clearly relate our predictions to the model parameters. Moreover, as we explained, this framework allows to capture the physics of possible UV completions, e.g. models of gauge-Higgs unification, in a simplified way. Due to the full consideration of a realistic (composite) lepton sector for the first time in the context of Higgs signals, we found a distinct phenomenology with respect to previous studies of composite models. In particular, we discovered generically a large reduction for the Higgs decay into two τ leptons in both setups considered, which is interesting in the light of the fact that a reduced τ -signal still fits well with the data

¹⁰We should stress that even for the more predictive and constrained 5D picture, we can still make the coupling of the SM fermions to the composite sector small without the need to reduce ξ . For instance, this can be achieved by UV localizing the corresponding fermions and thus making the interaction with the KK modes small.

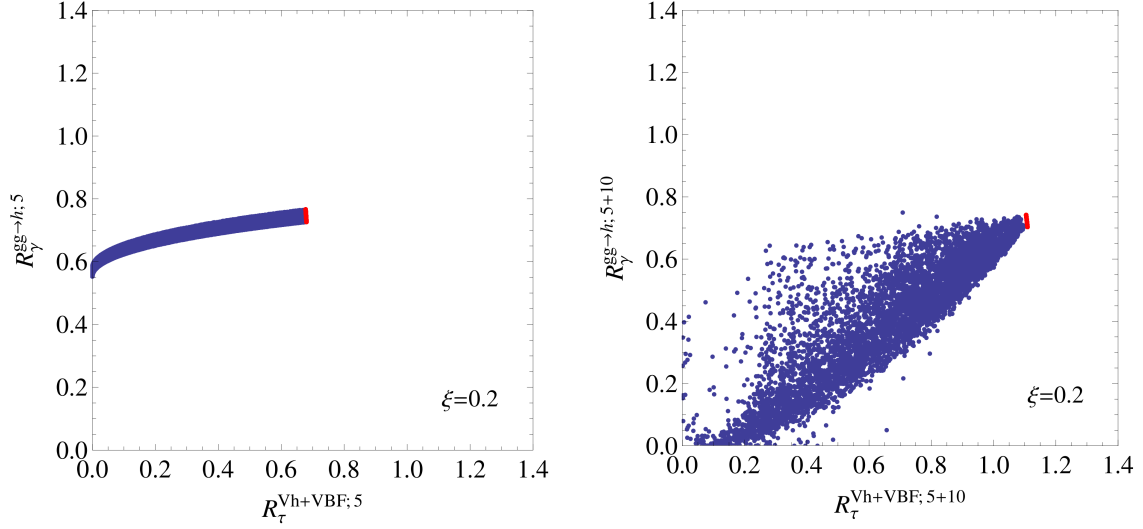


Figure 11. Left: Prediction for the production cross section times branching fraction for $gg \rightarrow h \rightarrow \gamma\gamma$ in the MCHM_5 including leading order effects from the non-linearity of the Higgs sector, relative to the SM versus the same ratio for $h \rightarrow \tau\tau$ in VBF or Vh production. The red region corresponds to the prediction neglecting the mixing with the composite lepton sector. Right: The analogous plot for the MCHM_{5+10} .

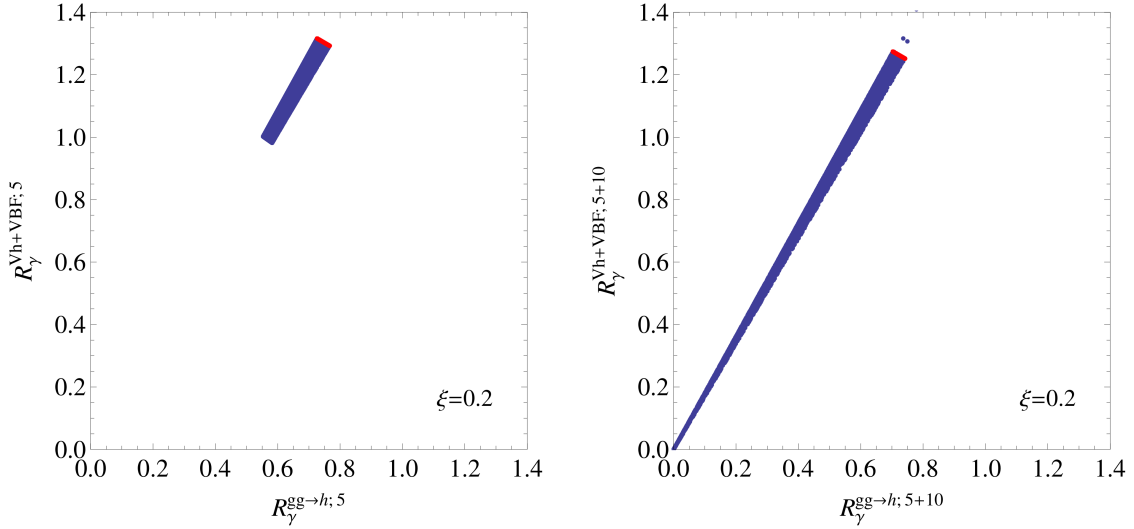


Figure 12. Left: Prediction for the production cross section times branching fraction for $gg \rightarrow h \rightarrow \gamma\gamma$ in the MCHM_5 with respect to the same decay if the Higgs has been produced in VBF or Vh production, including leading order effects from the non-linearity of the Higgs sector. The red region corresponds to the prediction neglecting the mixing with the composite lepton sector. Right: The analogous plot for the MCHM_{5+10} .

[3, 4]. On the other hand, neglecting possible UV completions, the new leptons of our framework of embedding the τ_R in a $\mathbf{10}$ of $SO(5)$ allow in principle for an enhancement in

the channel $pp \rightarrow h \rightarrow \gamma\gamma$, in agreement with current results from the LHC [3, 4]. If the experimental trend is confirmed, it would favor such an embedding with respect to the one of the MCHM₅.

However, considering the setups as the low energy theories of gauge-Higgs unification models, results in further constraints on their parameters [65]. For instance, this leads to the clear prediction of a reduced di-photon signal, due to the extended fermion sector, also in the model featuring a **10**, in analogy to the findings in the MCHM₅ (which had been independent of possible UV completions). The clear correlations found e.g. between the $\gamma\gamma$ and $\tau\tau$ channels, especially in the model corresponding to the MCHM₅, offer a nice possibility to discover or exclude the setups. We should notice here that additional effects arising from the non-linearity of the Higgs in complete composite models might lead to slight modifications of the previous picture like a possible enhancement for weak-boson induced processess. We have studied these effects in Section 3.4. Nevertheless, finding a slight reduction in the $gg \rightarrow h \rightarrow \gamma\gamma$ channel - which is still not excluded, considering the errors of current measurements - together with a depletion in the $h\tau\tau$ vertex could be interpreted as a hint for the compositeness of the τ lepton. Note that the phenomenology is different from the one of other extra-dimensional realizations of TeV-scale physics, like general Randall-Sundrum models [8, 76–81]. As we have seen that large signals are not to be expected from the quark sector (in tentative agreement with LHC measurements) it could be the unexpected compositeness of the τ lepton that leads to first signals of compositeness in Higgs physics at the LHC.

Addendum After completion of this work, new Higgs data were presented at the Moriond Conference [82]. While the significance of the excess in $pp \rightarrow h \rightarrow \gamma\gamma$ remained at the same level for the ATLAS experiment, the CMS results are now in agreement with the SM prediction within 1σ . Concerning the decay into τ leptons, the new ATLAS data are still consistent with a vanishing signal (with a reduced central value), whereas in CMS this decay mode has been established at the level of 3σ . For the latter experiment the central value is essentially at the SM prediction.

If the new CMS results on $pp \rightarrow h \rightarrow \gamma\gamma$ are confirmed by ATLAS, this would lead to a better agreement with the predictions of the considered (composite) UV completions of our low energy models, see e.g. Figure 11. However, if the $\tau\tau$ channel converges to the SM prediction, this would constrain significantly the scenarios studied in this work.

Acknowledgements We are grateful to Babis Anastasiou for stimulating discussions and Alex Azatov, Adam Falkowski, Giuliano Panico, as well as José Santiago for useful comments. The research of the authors is supported by the Swiss National Foundation under contract SNF 200021-143781.

A Form Factors

The form factors $A_{q,W}^h(\tau)$ which describe the effects of fermion and W^\pm -boson loops in the production and the decay of the Higgs boson are given by [69]

$$\begin{aligned} A_q^h(\tau) &= \frac{3\tau}{2} [1 + (1 - \tau) f(\tau)] , \\ A_W^h(\tau) &= -\frac{3}{4} [2 + 3\tau + 3\tau(2 - \tau) f(\tau)] . \end{aligned} \quad (\text{A.1})$$

The function $f(\tau)$ reads

$$f(\tau) = \begin{cases} -\frac{1}{4} \left[\ln \left(\frac{1 + \sqrt{1 - \tau}}{1 - \sqrt{1 - \tau}} \right) - i\pi \right]^2 , & \tau \leq 1 , \\ \arcsin^2 \left(\frac{1}{\sqrt{\tau}} \right) , & \tau > 1 . \end{cases} \quad (\text{A.2})$$

References

- [1] **ATLAS** Collaboration, G. Aad et al., *Observation of a new particle in the search for the Standard Model Higgs boson with the ATLAS detector at the LHC*, *Phys.Lett.* **B716** (2012) 1–29, [[arXiv:1207.7214](#)].
- [2] **CMS** Collaboration, S. Chatrchyan et al., *Observation of a new boson at a mass of 125 GeV with the CMS experiment at the LHC*, *Phys.Lett.* **B716** (2012) 30–61, [[arXiv:1207.7235](#)].
- [3] **ATLAS** Collaboration, *An update of combined measurements of the new higgs-like boson with high mass resolution channels*, *ATLAS-CONF-2012-170*.
- [4] **CMS** Collaboration, *Combination of standard model Higgs boson searches and measurements of the properties of the new boson with a mass near 125 GeV*, *CMS PAS HIG-12-045*.
- [5] A. Joglekar, P. Schwaller, and C. E. Wagner, *Dark Matter and Enhanced Higgs to Di-photon Rate from Vector-like Leptons*, *JHEP* **1212** (2012) 064, [[arXiv:1207.4235](#)].
- [6] N. Arkani-Hamed, K. Blum, R. T. D’Agnolo, and J. Fan, *2:1 for Naturalness at the LHC?*, *JHEP* **1301** (2013) 149, [[arXiv:1207.4482](#)].
- [7] U. Ellwanger, *A Higgs boson near 125 GeV with enhanced di-photon signal in the NMSSM*, *JHEP* **1203** (2012) 044, [[arXiv:1112.3548](#)].
- [8] F. Goertz, U. Haisch, and M. Neubert, *Bounds on Warped Extra Dimensions from a Standard Model-like Higgs Boson*, *Phys.Lett.* **B713** (2012) 23–28, [[arXiv:1112.5099](#)].
- [9] K. Blum and R. T. D’Agnolo, *2 Higgs or not 2 Higgs*, *Phys.Lett.* **B714** (2012) 66–69, [[arXiv:1202.2364](#)].
- [10] J.-J. Cao, Z.-X. Heng, J. M. Yang, Y.-M. Zhang, and J.-Y. Zhu, *A SM-like Higgs near 125 GeV in low energy SUSY: a comparative study for MSSM and NMSSM*, *JHEP* **1203** (2012) 086, [[arXiv:1202.5821](#)].
- [11] F. Boudjema and G. D. La Rochelle, *Beyond the MSSM Higgs bosons at 125 GeV*, *Phys.Rev.* **D86** (2012) 015018, [[arXiv:1203.3141](#)].
- [12] L. Wang and X.-F. Han, *LHC diphoton Higgs signal and top quark forward-backward asymmetry in quasi-inert Higgs doublet model*, *JHEP* **1205** (2012) 088, [[arXiv:1203.4477](#)].

- [13] B. Bellazzini, C. Csaki, J. Hubisz, J. Serra, and J. Terning, *Composite Higgs Sketch*, *JHEP* **1211** (2012) 003, [[arXiv:1205.4032](#)].
- [14] S. Dawson and E. Furlan, *A Higgs Conundrum with Vector Fermions*, *Phys.Rev.* **D86** (2012) 015021, [[arXiv:1205.4733](#)].
- [15] A. Azatov, S. Chang, N. Craig, and J. Galloway, *Higgs fits preference for suppressed down-type couplings: Implications for supersymmetry*, *Phys.Rev.* **D86** (2012) 075033, [[arXiv:1206.1058](#)].
- [16] N. Bonne and G. Moreau, *Reproducing the Higgs boson data with vector-like quarks*, *Phys.Lett.* **B717** (2012) 409–419, [[arXiv:1206.3360](#)].
- [17] K. Hagiwara, J. S. Lee, and J. Nakamura, *Properties of 125 GeV Higgs boson in non-decoupling MSSM scenarios*, *JHEP* **1210** (2012) 002, [[arXiv:1207.0802](#)].
- [18] B. Bellazzini, C. Petersson, and R. Torre, *Photophilic Higgs from sgoldstino mixing*, *Phys.Rev.* **D86** (2012) 033016, [[arXiv:1207.0803](#)].
- [19] R. Benbrik, M. Gomez Bock, S. Heinemeyer, O. Stal, G. Weiglein, et al., *Confronting the MSSM and the NMSSM with the Discovery of a Signal in the two Photon Channel at the LHC*, *Eur.Phys.J.* **C72** (2012) 2171, [[arXiv:1207.1096](#)].
- [20] M. R. Buckley and D. Hooper, *Are There Hints of Light Stops in Recent Higgs Search Results?*, *Phys.Rev.* **D86** (2012) 075008, [[arXiv:1207.1445](#)].
- [21] H. An, T. Liu, and L.-T. Wang, *125 GeV Higgs Boson, Enhanced Di-photon Rate, and Gauged $U(1)_{PQ}$ -Extended MSSM*, *Phys.Rev.* **D86** (2012) 075030, [[arXiv:1207.2473](#)].
- [22] A. Alves, E. Ramirez Barreto, A. Dias, C. de S. Pires, F. S. Queiroz, et al., *Explaining the Higgs Decays at the LHC with an Extended Electroweak Model*, *Eur.Phys.J.* **C73** (2013) 2288, [[arXiv:1207.3699](#)].
- [23] T. Abe, N. Chen, and H.-J. He, *LHC Higgs Signatures from Extended Electroweak Gauge Symmetry*, *JHEP* **1301** (2013) 082, [[arXiv:1207.4103](#)].
- [24] D. Bertolini and M. McCullough, *The Social Higgs*, *JHEP* **1212** (2012) 118, [[arXiv:1207.4209](#)].
- [25] N. Craig and S. Thomas, *Exclusive Signals of an Extended Higgs Sector*, *JHEP* **1211** (2012) 083, [[arXiv:1207.4835](#)].
- [26] L. G. Almeida, E. Bertuzzo, P. A. Machado, and R. Z. Funchal, *Does $H \rightarrow \gamma\gamma$ Taste like vanilla New Physics?*, *JHEP* **1211** (2012) 085, [[arXiv:1207.5254](#)].
- [27] B. Batell, D. McKeen, and M. Pospelov, *Singlet Neighbors of the Higgs Boson*, *JHEP* **1210** (2012) 104, [[arXiv:1207.6252](#)].
- [28] M. Hashimoto and V. Miransky, *Enhanced diphoton Higgs decay rate and isospin symmetric Higgs boson*, *Phys.Rev.* **D86** (2012) 095018, [[arXiv:1208.1305](#)].
- [29] K. Schmidt-Hoberg and F. Staub, *Enhanced $h \rightarrow \gamma\gamma$ rate in MSSM singlet extensions*, *JHEP* **1210** (2012) 195, [[arXiv:1208.1683](#)].
- [30] M. Reece, *Vacuum Instabilities with a Wrong-Sign Higgs-Gluon-Gluon Amplitude*, *New J.Phys.* **15** (2013) 043003, [[arXiv:1208.1765](#)].
- [31] F. Boudjema and G. D. La Rochelle, *Supersymmetric Higgses beyond the MSSM: An update with flavour and Dark Matter constraints*, *Phys.Rev.* **D86** (2012) 115007, [[arXiv:1208.1952](#)].

- [32] L. Wang and X.-F. Han, *130 GeV gamma-ray line and enhancement of $h \rightarrow \gamma\gamma$ in the Higgs triplet model plus a scalar dark matter*, *Phys.Rev.* **D87** (2013) 015015, [[arXiv:1209.0376](#)].
- [33] A. Alves, *Is the New Resonance Spin 0 or 2? Taking a Step Forward in the Higgs Boson Discovery*, *Phys.Rev.* **D86** (2012) 113010, [[arXiv:1209.1037](#)].
- [34] E. Bertuzzo, P. A. Machado, and R. Zukanovich Funchal, *Can New Colored Particles Illuminate the Higgs?*, *JHEP* **1302** (2013) 086, [[arXiv:1209.6359](#)].
- [35] M. Chala, *$h \rightarrow \gamma\gamma$ excess and Dark Matter from Composite Higgs Models*, *JHEP* **1301** (2013) 122, [[arXiv:1210.6208](#)].
- [36] S. Dawson, E. Furlan, and I. Lewis, *Unravelling an extended quark sector through multiple Higgs production?*, *Phys.Rev.* **D87** (2013) 014007, [[arXiv:1210.6663](#)].
- [37] U. Haisch and F. Mahmoudi, *MSSM: Cornered and Correlated*, *JHEP* **1301** (2013) 061, [[arXiv:1210.7806](#)].
- [38] P. Bechtle, S. Heinemeyer, O. Stal, T. Stefaniak, G. Weiglein, et al., *MSSM Interpretations of the LHC Discovery: Light or Heavy Higgs?*, *Eur.Phys.J.* **C73** (2013) 2354, [[arXiv:1211.1955](#)].
- [39] C. Petersson, A. Romagnoni, and R. Torre, *Liberating Higgs couplings in supersymmetry*, *Phys.Rev.* **D87** (2013) 013008, [[arXiv:1211.2114](#)].
- [40] K. Schmidt-Hoberg, F. Staub, and M. W. Winkler, *Enhanced diphoton rates at Fermi and the LHC*, *JHEP* **1301** (2013) 124, [[arXiv:1211.2835](#)].
- [41] E. Dudas, C. Petersson, and P. Tziveloglou, *Low Scale Supersymmetry Breaking and its LHC Signatures*, *Nucl.Phys.* **B870** (2013) 353–383, [[arXiv:1211.5609](#)].
- [42] M. Berg, I. Buchberger, D. Ghilencea, and C. Petersson, *Higgs diphoton rate enhancement from supersymmetric physics beyond the MSSM*, *Phys.Rev.* **D88** (2013) 025017, [[arXiv:1212.5009](#)].
- [43] E. Ilhan, *Higgs to diphoton decay rate and the antisymmetric tensor unparticle mediation*, *Acta Phys.Polon.* **B44** (2013) 1287–1295, [[arXiv:1212.5695](#)].
- [44] W. Chao, J.-H. Zhang, and Y. Zhang, *Vacuum Stability and Higgs Diphoton Decay Rate in the Zee-Babu Model*, *JHEP* **1306** (2013) 039, [[arXiv:1212.6272](#)].
- [45] C. Han, N. Liu, L. Wu, J. M. Yang, and Y. Zhang, *Two-Higgs-doublet model with a color-triplet scalar: a joint explanation for top quark forward-backward asymmetry and Higgs decay to diphoton*, [arXiv:1212.6728](#).
- [46] E. J. Chun and P. Sharma, *A light triplet boson and Higgs-to-diphoton in supersymmetric type II seesaw*, *Phys.Lett.* **B722** (2013) 86–93, [[arXiv:1301.1437](#)].
- [47] S. Funatsu, H. Hatanaka, Y. Hosotani, Y. Orikasa, and T. Shimotani, *Novel universality and Higgs decay $H \rightarrow \gamma\gamma$, gg in the $SO(5) \times U(1)$ gauge-Higgs unification*, *Phys.Lett.* **B722** (2013) 94–99, [[arXiv:1301.1744](#)].
- [48] C. Grojean, E. E. Jenkins, A. V. Manohar, and M. Trott, *Renormalization Group Scaling of Higgs Operators and $\Gamma(h \rightarrow \gamma\gamma)$* , *JHEP* **1304** (2013) 016, [[arXiv:1301.2588](#)].
- [49] J. Fan and M. Reece, *Probing Charged Matter Through Higgs Diphoton Decay, Gamma Ray Lines, and EDMs*, *JHEP* **1306** (2013) 004, [[arXiv:1301.2597](#)].
- [50] N. Manton, *A New Six-Dimensional Approach to the Weinberg-Salam Model*, *Nucl.Phys.* **B158** (1979) 141.

- [51] H. Hatanaka, T. Inami, and C. Lim, *The Gauge hierarchy problem and higher dimensional gauge theories*, *Mod.Phys.Lett.* **A13** (1998) 2601–2612, [[hep-th/9805067](#)].
- [52] G. von Gersdorff, N. Irges, and M. Quiros, *Bulk and brane radiative effects in gauge theories on orbifolds*, *Nucl.Phys.* **B635** (2002) 127–157, [[hep-th/0204223](#)].
- [53] C. Csaki, C. Grojean, and H. Murayama, *Standard model Higgs from higher dimensional gauge fields*, *Phys.Rev.* **D67** (2003) 085012, [[hep-ph/0210133](#)].
- [54] R. Contino, Y. Nomura, and A. Pomarol, *Higgs as a holographic pseudo-Goldstone boson*, *Nucl. Phys.* **B671** (2003) 148–174, [[hep-ph/0306259](#)].
- [55] K. Agashe, R. Contino, and A. Pomarol, *The Minimal Composite Higgs Model*, *Nucl. Phys.* **B719** (2005) 165–187, [[hep-ph/0412089](#)].
- [56] M. S. Carena, E. Ponton, J. Santiago, and C. E. Wagner, *Light Kaluza Klein States in Randall-Sundrum Models with Custodial $SU(2)$* , *Nucl.Phys.* **B759** (2006) 202–227, [[hep-ph/0607106](#)].
- [57] M. S. Carena, E. Ponton, J. Santiago, and C. Wagner, *Electroweak constraints on warped models with custodial symmetry*, *Phys.Rev.* **D76** (2007) 035006, [[hep-ph/0701055](#)].
- [58] R. Contino, L. Da Rold, and A. Pomarol, *Light custodians in natural composite Higgs models*, *Phys.Rev.* **D75** (2007) 055014, [[hep-ph/0612048](#)].
- [59] M. Carena, A. D. Medina, B. Panes, N. R. Shah, and C. E. Wagner, *Collider phenomenology of gauge-Higgs unification scenarios in warped extra dimensions*, *Phys.Rev.* **D77** (2008) 076003, [[arXiv:0712.0095](#)].
- [60] A. Pomarol and J. Serra, *Top Quark Compositeness: Feasibility and Implications*, *Phys.Rev.* **D78** (2008) 074026, [[arXiv:0806.3247](#)].
- [61] G. Panico, M. Safari, and M. Serone, *Simple and Realistic Composite Higgs Models in Flat Extra Dimensions*, *JHEP* **1102** (2011) 103, [[arXiv:1012.2875](#)].
- [62] O. Matsedonskyi, G. Panico, and A. Wulzer, *Light Top Partners for a Light Composite Higgs*, *JHEP* **1301** (2013) 164, [[arXiv:1204.6333](#)].
- [63] F. del Aguila, A. Carmona, and J. Santiago, *Neutrino Masses from an A_4 Symmetry in Holographic Composite Higgs Models*, *JHEP* **1008** (2010) 127, [[arXiv:1001.5151](#)].
- [64] F. del Aguila, A. Carmona, and J. Santiago, *Tau Custodian searches at the LHC*, *Phys.Lett.* **B695** (2011) 449–453, [[arXiv:1007.4206](#)].
- [65] A. Carmona and F. Goertz *Work in progress*.
- [66] A. Atre, M. Carena, T. Han, and J. Santiago, *Heavy Quarks Above the Top at the Tevatron*, *Phys.Rev.* **D79** (2009) 054018, [[arXiv:0806.3966](#)].
- [67] A. Atre, G. Azuelos, M. Carena, T. Han, E. Ozcan, et al., *Model-Independent Searches for New Quarks at the LHC*, *JHEP* **1108** (2011) 080, [[arXiv:1102.1987](#)].
- [68] K. Agashe, R. Contino, L. Da Rold, and A. Pomarol, *A Custodial symmetry for Zb anti- b* , *Phys.Lett.* **B641** (2006) 62–66, [[hep-ph/0605341](#)].
- [69] A. Djouadi, *The Anatomy of electro-weak symmetry breaking. I: The Higgs boson in the standard model*, *Phys.Rept.* **457** (2008) 1–216, [[hep-ph/0503172](#)].
- [70] **ATLAS** Collaboration, *Search for heavy top-like quarks decaying to a higgs boson and a top*

quark in the lepton plus jets final state in pp collisions at $\sqrt{s} = 8$ tev with the atlas detector, Tech. Rep. ATLAS-CONF-2013-018, CERN, Geneva, Mar, 2013.

- [71] A. Falkowski, *Pseudo-goldstone Higgs production via gluon fusion*, *Phys.Rev.* **D77** (2008) 055018, [[arXiv:0711.0828](#)].
- [72] A. Azatov and J. Galloway, *Light Custodians and Higgs Physics in Composite Models*, *Phys.Rev.* **D85** (2012) 055013, [[arXiv:1110.5646](#)].
- [73] E. Furlan, *Gluon-fusion Higgs production at NNLO for a non-standard Higgs sector*, *JHEP* **1110** (2011) 115, [[arXiv:1106.4024](#)].
- [74] F. del Aguila, M. Perez-Victoria, and J. Santiago, *Observable contributions of new exotic quarks to quark mixing*, *JHEP* **0009** (2000) 011, [[hep-ph/0007316](#)].
- [75] G. Giudice, C. Grojean, A. Pomarol, and R. Rattazzi, *The Strongly-Interacting Light Higgs*, *JHEP* **0706** (2007) 045, [[hep-ph/0703164](#)].
- [76] A. Djouadi and G. Moreau, *Higgs production at the LHC in warped extra-dimensional models*, *Phys.Lett.* **B660** (2008) 67–71, [[arXiv:0707.3800](#)].
- [77] A. Azatov, M. Toharia, and L. Zhu, *Higgs Mediated FCNC's in Warped Extra Dimensions*, *Phys.Rev.* **D80** (2009) 035016, [[arXiv:0906.1990](#)].
- [78] C. Bouchart and G. Moreau, *Higgs boson phenomenology and VEV shift in the RS scenario*, *Phys.Rev.* **D80** (2009) 095022, [[arXiv:0909.4812](#)].
- [79] S. Casagrande, F. Goertz, U. Haisch, M. Neubert, and T. Pfoh, *The Custodial Randall-Sundrum Model: From Precision Tests to Higgs Physics*, *JHEP* **1009** (2010) 014, [[arXiv:1005.4315](#)].
- [80] A. Azatov, M. Toharia, and L. Zhu, *Higgs Production from Gluon Fusion in Warped Extra Dimensions*, *Phys.Rev.* **D82** (2010) 056004, [[arXiv:1006.5939](#)].
- [81] M. Carena, S. Casagrande, F. Goertz, U. Haisch, and M. Neubert, *Higgs Production in a Warped Extra Dimension*, *JHEP* **1208** (2012) 156, [[arXiv:1204.0008](#)].
- [82] *See talks given at the “48th Rencontres de Moriond (2013)”*,
<https://indico.in2p3.fr/conferenceDisplay.py?confId=7411>,
<http://moriond.in2p3.fr/QCD/2013/qcd.html>.